UNIVERSITÄT DUISBURG ESSEN

Offen im Denken

Final Report for:

Investigation of Membrane Fouling in the Treatment of Oily Wastewater: Influence of Surfactants and Co-Surfactants (W-UFO II)

Reporting period:
September 2020 - October 2021

Team:

University of Duisburg-Essen
Faculty of Engineering
Department of Mechanical Engineering and Process Engineering
Chair of Mechanical Process Engineering / Water Technology

Lotharstr. 1

47057 Duisburg

www.uni-due.de/wassertechnik/

Prof. Dr.-Ing. Stefan Panglisch (Project PI)
Telefon: 0203 379 -3477
stefan.panglisch@uni-due.de

Dr. rer. Nat. Ibrahim ElSherbiny
ibrahim.elsherbiny@uni-due.de

M.Sc. Hasan Idrees
hasan.idrees@uni-due.de

Project funding by the

Willy-Hager Stiftung
c/o Technische Universität Kaiserslautern
Paul-Ehrlich-Straße 14
67663 Kaiserslautern

Contact:
Prof. Dr.-Ing. Heidrun Steinmetz

Contents

List of abbreviations

Am	Membrane active surface area
CF	Constant flux
CMC	Critical micelle concentration
CP	Constant pressure
CTAB	Cetyltrimethylammonium bromide
d_{32}	Sauter mean diameter
DI	Pure water
FS	Flat sheet UF membranes
GC-FID	Gas chromatography – flame ionization detector
HF	Hollow fiber membranes
HLB	Hydrophilic-lipophilic balance
HPH	High-pressure homogenizer
J	Filtration flux
MM	Modified hollow fiber membrane model
MWCO	Molecular wight cut-off
NP	Normalized permeability
OWWE	Produced water after primary and secondary treatment stages
PAH	Polycyclic aromatic hydrocarbons
PES	Polyether sulfone
P_m	Membrane permeability
P_{W0}	Initial pure water permeability
Q	Filtered volume rate per unit time
SDS	Sodium Dodecyl sulfate
SEM	Scanning electron microscope
SM	Standard hollow fiber membrane model
TMP	Transmembrane pressure
TOC	Total organic carbon
UF	Ultrafiltration
US-EPA	United states environmental protection agency

1 Introduction and project objectives

The ultimate objective of W-UFO research project series is to establish an efficient pressure-driven membrane-based treatment for the purification of produced water, which is based on employing polymeric ultrafiltration (UF) membranes in dead-end operation. This is targeted as a polishing step in the treatment process of oily wastewater effluents (i.e., produced water after primary and secondary treatment stages, hereafter abbreviated as OWWE). Here, the oil concentration is usually in the range of 20 - 100 mg/L, and the average oil droplet size is commonly below 1 µm. To achieve that, it is essential to gather a deep understanding of UF membrane performance during filtration of different oil-contaminated feeds at different operating conditions, as well as the accompanied fouling mechanisms. W-UFO research plan was divided into four subprojects (named as W-UFO I – IV). In this report, the main achievements of W-UFO II are presented, besides some correlations to the outputs of W-UFO I are also mentioned in the respective sections.

According to the original research plan (see W-UFO II proposal, page 5), W-UFO I aimed at studying the influence of oil droplet size distribution on fouling mechanisms and coalescence phenomena, as well as the influence of salts in the feed solution on the stability of oil nano-emulsions[1] and the fouling mechanisms The results of the first sub-project, which was completed on 31.07.2019, are presented in the associated final report(Idrees, ElSherbiny, & Panglisch, 2019). W-UFO II focused on the impacts of using surfactants and co-surfactants on the stability of oil nano-emulsions, UF membrane performance and fouling mechanisms. W-UFO III was originally planned to first focus on the quantification of dissolved oil in OWWE and studying its influence on UF membrane performance and fouling behavior, and second to enhance the treatment efficiency via dosing of powdered activated carbon and/or flocculants (prior to membrane filtration). W-UFO IV was planned to combine the outputs of the three subprojects for the optimization of the main operating parameters in OWWE treatment

[1] Emulsions with droplets below 1 µm have been called by various names in the literature, e.g. micro-emulsions, nano-emulsions, ultrafine emulsions, submicron emulsions, emulsoids or mini-emulsions. Recently they are mainly described as micro- or nano-emulsions. According to common terminology, the main differences between micro-emulsions and nano-emulsions are thermodynamic or the kinetic stability. In general, micro-emulsions are thermodynamically stable and isotropic emulsions. Nano-emulsions have lower thermodynamic and kinetic stability. The model emulsions used in this study have different compositions and mixing ratios of oil, water, surfactants, co-surfactants and salts. This does not guarantee that they are thermodynamically stable. Therefore, and to avoid confusion, the emulsions prepared will be referred to as as nano-emulsions in the further course of the report.

process (i.e., membrane flux, filtration mode, filtration cycle duration and backwashing frequencies). Semi-technical scale experiments using real OWWE were planned as well. The latter two sub-projects have been combined in one project, W-UFO III^{+}, which was recently approved by the Willy-Hager Foundation.

2 W-UFO II progress summary and modifications to the original plan

W-UFO II was launched in September 2020. All work packages were started at the respective times, according to the work plan. In WP1, the model oil feed solutions mimicking OWWE were prepared, thereafter filtration tests using both flat sheet and hollow fiber (or capillary) UF membranes were started as planned in WP2. In parallel, the experimental results were processed and analyzed as planned in WP3. Nevertheless, due to the COVID-19 conditions in the fall of 2020 and early 2021, university access and lab capacity were significantly limited, resulting in a delay in the progress of WP2 and WP3 in 2021. Therefore, W-UFO II was extended for 2 months (until October 2021).

3 Main scientific and technical outputs

3.1 Material and methods

3.1.1 Chemicals

For oil-in-water nano-emulsions preparation, a standard light crude oil (AR-2048, 2.01 wt.% Sulfur), produced by Alpha Resources LLC, USA, was employed to ensure a reproducible source of oil. The content of polycyclic aromatic hydrocarbons (PAH) in the crude oil was analyzed using Gas Chromatography – Flame Ionization Detector (GC-FID), according to the US-EPA 16 PAH list with a determination limit of 3 mg/L, by the organic analysis department at IWW water center, Mülheim an der Ruhr. The PAH contents are shown in **Table 1**.

Pure water (DI) was provided by a reverse osmosis water system (Model: Osmose 190, Denerle, Germany) with a permeate quality (conductivity: ~ 35 µS/cm, dissolved organic carbon content: < 0.2 ppm). Ethanol (96% denatured), purchased from Carl Roth® GmbH, was employed for flat membranes cleaning. Sodium hydroxide (NaOH) and sodium hypochlorite (NaOCl) were obtained from VWR International. Sodium dodecyl sulfate (SDS; molecular weight 288.38 Da; anionic surfactant), polysorbate 20 (Tween® 20; molecular weight 1,227.72 Da; nonionic surfactant),

cetyltrimethylammonium bromide (CTAB; molecular weight 364.45 Da; cationic surfactant) and 2-pentanol (molecular weight 88.15 Da; co-surfactant) were utilized as emulsifiers.

Table 1: Composition of polycyclic aromatic hydrocarbon (PAH) in crude oil, measured using GC-FID, according to the US-EPA 16 PAH list; < 3 means that the value was below the limit of determination

PAH components	Conc. in mg/L	PAH components	Conc. in mg/L
Acenaphthen	<3	Acenaphthylen	<3
Dibenz[a,h]anthracen	<3	Anthracen	<3
Fluoranthen	<3	Benzo[a]anthracen	35
Fluoren	<3	Benzo[a]pyren	<3
Indeno[1,2,3-c,d]pyren	<3	Benzo[b]fluoranthen	<3
Naphthalin	620	Benzo[ghi]perylen	<3
Phenanthren	150	Benzo[k]fluoranthen	<3
Pyren	3	Chrysen	<3

Reef salt artificial seawater salts (ASW) were purchased from Aquamedic, Germany. The main components of the reef salt are listed in **Table 2.**

Table 2: Major components of reef salt artificial seawater salts

Element	Conc. in g/kg	Element	Conc. in g/kg
Na^+	254	Cl^-	488
Mg^{2+}	30	SO_4^{-2}	60
Ca^{2+}	11	HCO_3^-/CO_3^{2-}	4
K^+	10	H_2O	142

3.1.2 Membranes

Two types of polyether sulfone (PES) flat sheet UF membranes (FS) were tested in this work; Nadir® UP150 P and Trisep® UB50, both from Mann+Hummel, Germany (previously known as “Micodyn Nadir”). FS membranes exhibited molecular weight cut-off (MWCO) of about 150 and 50 kDa for UP150 and UB50, respectively. FS were implemented in form of discs with active surface area of ~ 13.8 cm². Multibore® hollow fiber (HF) membranes with an average barrier pore diameter of 20 nm were obtained from inge GmbH, Germany, were also implemented in this study. The used HF membrane modules had an active surface area of 510 cm².

Scanning Electron Microscope (SEM) (FEI, USA) was used to analyze the cross section and top surface morphologies of pristine and fouled membranes at standard high vacuum conditions. Samples were coated with silver using a K-550 sputter coater

(Emitech, U.K.). Samples were sputtered for 1.5 min in case of cross section analysis and for 0.5 min for the surface scan.

3.1.3 Preparation of synthetic oily feed water (model oil feed emulsions)

3.1.3.1 Homogenizers

Based on the outputs of W-UFO I, a high-pressure homogenizer was found to be the most effective tool to produce nano-emulsions with small and stable oil droplets of sizes in range of 500 nm. Nevertheless, prior to HPH, crude oil and water were pre-mixed using stator-rotor mixer.

3.1.3.1.1 Stator-rotor mixer

For premixing crude oil in water, a high-speed stator-rotor mixer Ultra-Turrax® T25 (IKA-Werke GmbH & Co. KG, Germany, **Figure 1**) was employed to produce fine homogenized oil-water mixture prior to HPH.

Figure 1: Stator-rotor mixer, Ultra-turrax T25 IKA®

Ultra-Turrax® T25 is designed for dispersing and emulsifying liquid media in batch operation with a maximal energy output of 350 Watt.

3.1.3.1.2 High pressure homogenizer

The high-pressure homogenizer (HPH), see **Figure 2**Fehler! Verweisquelle konnte nicht gefunden werden.**,** is an inline dispersing machine used for continuous production of superfine emulsions, even nano-emulsions. The HPH (by IKA®-Werke GmbH & Co. KG, Germany) consists of a feed emulsion container, a working chamber, a high-pressure piston pump, in addition to other components, e.g., barometers, control valves and high-pressure pipes. During homogenizing, high pressure is generated by the reduced cross-section in the homogenizing valve, thereafter strong turbulent streams are

generated by releasing of the high pressure in a very narrow adjustable gab of the valve. Subsequently, these strong turbulent streams can perfect homogenization of oil-water mixtures.

Figure 2: High Pressure Homogenizer (HPH), manufactured by IKA®-Werke GmbH & Co. KG, Germany

3.1.3.2 Analytics

3.1.3.2.1 Oil droplet size distribution

The model feed waters were characterized in terms of oil droplet size distribution using a laser diffraction particle size analyzer (Model: LS 13320, Beckman Coulter, USA, cf. **Figure 3**). It measures the particle size distribution of dispersed materials in the liquid state based in the of range of 0.017 to 2,000 µm.

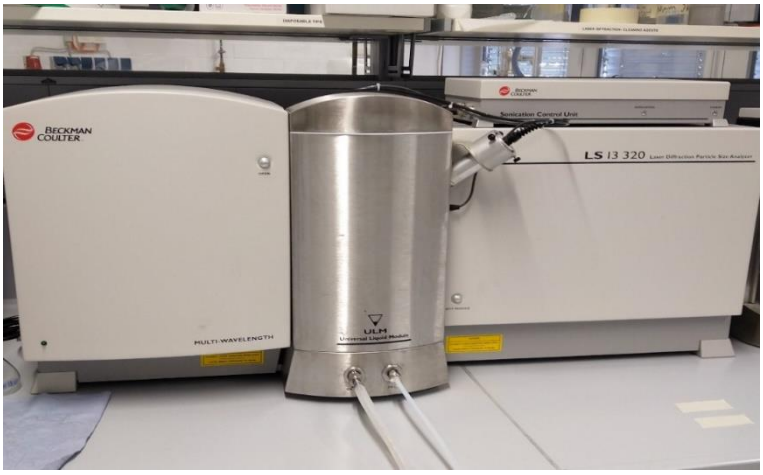

Figure 3: Coulter Beckman LS 13 320 Laser Diffraction particle size analyzer

3.1.3.2.2 TOC, pH and conductivity

The oil content of the prepared oily feeds was also determined by measuring the total organic carbon (TOC) by TOC-L device (Shmidazu, Japan, **cf. Figure 4**), which was calibrated with potassium hydrogen phthalate. Calibration has been split into two ranges (1 – 10 mg/L; 20 – 100 mg/L) to increase the accuracy of the measurement. The confidence interval (confidence level 95%) was calculated according to Funk et al, 2005 (Funk, Dammann, & Donnevert, 2005), the limit of determination was calculated according to DIN 32645. **Table 3** indicates the confidence interval and the limit of determination for TOC measurement.

Table 3: The confidence interval and the determination limit for TOC measurement with Shimadzu TOC-L device

TOC measurement range in mg/L	Confidence interval in mg/L	Limit of determination in mg/L
1 – 10	±0.14	0.5
20 – 100	±0.8	3

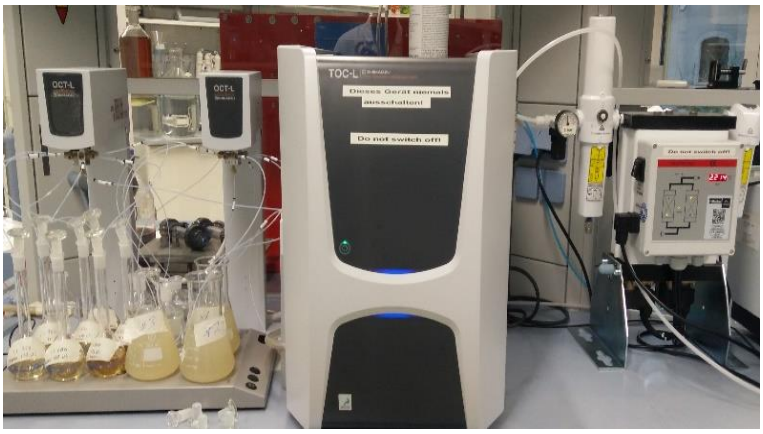

Figure 4: Shimazu TOC-L, TOC measurement device

The pH-value and conductivity of model feed water and permeate were measured using PH 197i (WTW) and Cond 197i (WTW), respectively (**cf. Figure 5**).

Figure 5: PH 197i pH meter, WTW (Left) and Cond 197i conductivity meter, WTW (right)

3.1.3.3 Preparation of oil-in-water nano-emulsions

Nano-emulsions of different oil concentration of 5 – 50 ppm were produced using the HPH. Crude oil and DI water were mixed at oil/water volumetric ratio of 1/250, and initially homogenized by Ultra-Turrax® for one minute to produce so called “Pre-mix”. This was further homogenized by the HPH at a pressure of ~1,000 bar to get a nano-emulsion via two emulsification passes. Since the final target is to simulate the feed of the polishing step in oily wastewater treatment, OWWE, particles bigger than 10 µm were removed in a fining step via typical filtration through filter papers with a minimum and maximum pore size of 25 and 60 µm, respectively (qualitative filter papers, grade: 310, VWR international, cf. **Figure 6**).

Figure 6: Qualitative filter paper, grade: 310, VWR international (left) and the final nano-emulsion (right)

3.1.3.4 Preparation of synthetic oil feed water for filtration experiments

According to the research plan of W-UFO II, different synthetic model feed waters were prepared to examine the impacts of surfactants and co-surfactant types and concentrations on the membrane fouling at different oil concentrations and with and without salts. Subsequently, different surfactant concentrations were employed, 0.2, 0.5 and 1 CMC (critical micelle concentration), where 1 CMC equals to ~2.4, 0.074 and 0.333 g/L in case of SDS, Tween 20 and CTAB, respectively. The co-surfactant, 2-pentanol, was used at a constant weight ratio of 7:6 (surfactant: 2-pentanol). ASW was used at constant concentration of 3.5 g/L. A complete list of filtration experiments in W-UFO II along with composition of the model oil feed waters that were carried out using UP150 P membranes is presented in Table A 1 in page 43 in the appendix together with the filtration curves of each single experiment.

Prior to filtration experiments, the prepared nano-emulsions were analyzed to examine the impact of additives on oil droplet size distribution. As indicated in **Figure 7,** oil nano-

emulsions containing light crude-oil and water only (i.e., without adding surfactants, co-surfactant, or salts, labeled as “without additives”) were found to exhibit an oil droplet size distribution in the range of 0.1 – 10 µm with a Sauter mean diameter d_{32} = 0.58 µm. Moreover, measurement of oil nano-emulsions with different surfactant concentrations revealed no significant changes in the oil droplet size distribution. For instance, oil nano-emulsions with different concentrations of 0.2, 0.5 and 1 CMC (cf. **Figure 7 A**) exhibited a Sauter mean diameter d_{32} of 0.64, 0.58 and 0.48 µm, respectively. Similarly, d_{32} of 0.62 and 0.64 µm were measured for oil nano-emulsions with Tween 20 and CTAB at a concentration of 1 CMC (**Figure 7 B**), respectively.

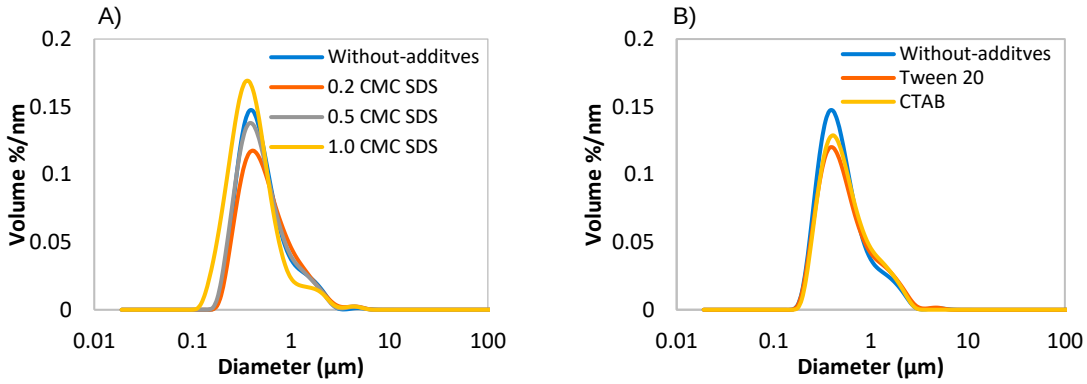

Figure 7: Differential volume size distribution of oil nano-emulsions with (A) without additives, and SDS concentrations of 0.2, 0.5 and 1 CMC, (B) different surfactants Tween 20 and CTAB at concentrations of 1 CMC

3.1.4 Bench- and lab-scale filtration experiments

3.1.4.1 Filtration systems

Filtration tests in dead-end mode were conducted using two bench-scale and one lab-scale membrane testing unit. As schematically represented in **Figure 8** and shown in **Figure 9**, the first bench-scale testing unit, assembled by convergence B.V. (Netherlands), is a fully-automated system that can be operated at constant pressure (up to 6 bar) and constant flux conditions (constant flow rate up to 2 L/h).

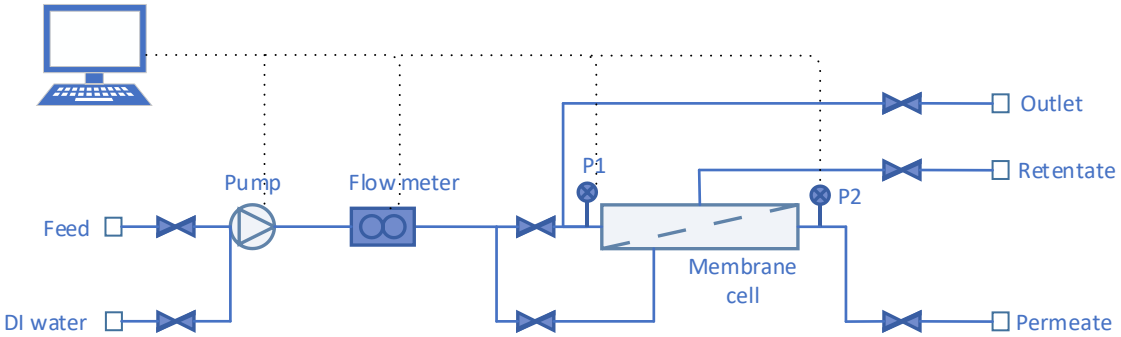

Figure 8: Schematic representation of the bench-scale dead-end filtration unit at constant flow rate for flat-sheet membranes

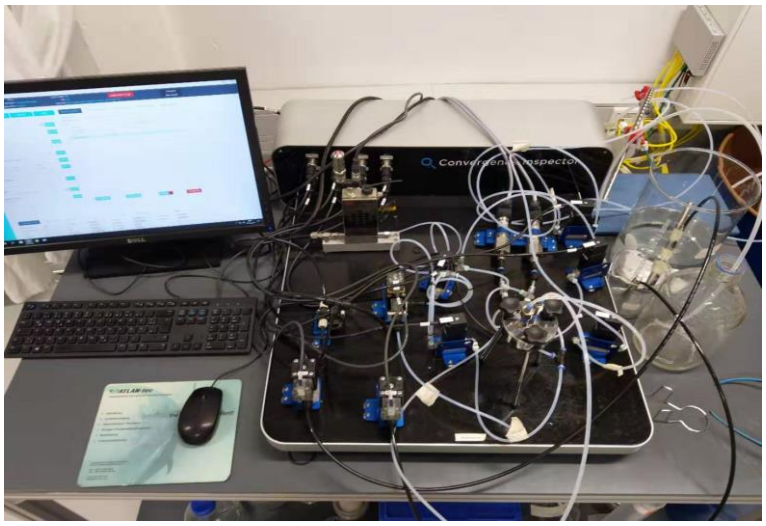

Figure 9: Bench-scale dead-end filtration unit at constant flow rate for flat-sheet membranes

For this system a membrane holder, from Tami membranes, France, with different support layers were employed. For PES FS membranes, spiral rubber support layer, metal screen and paraffin screen were installed, as shown in **Figure 10.**

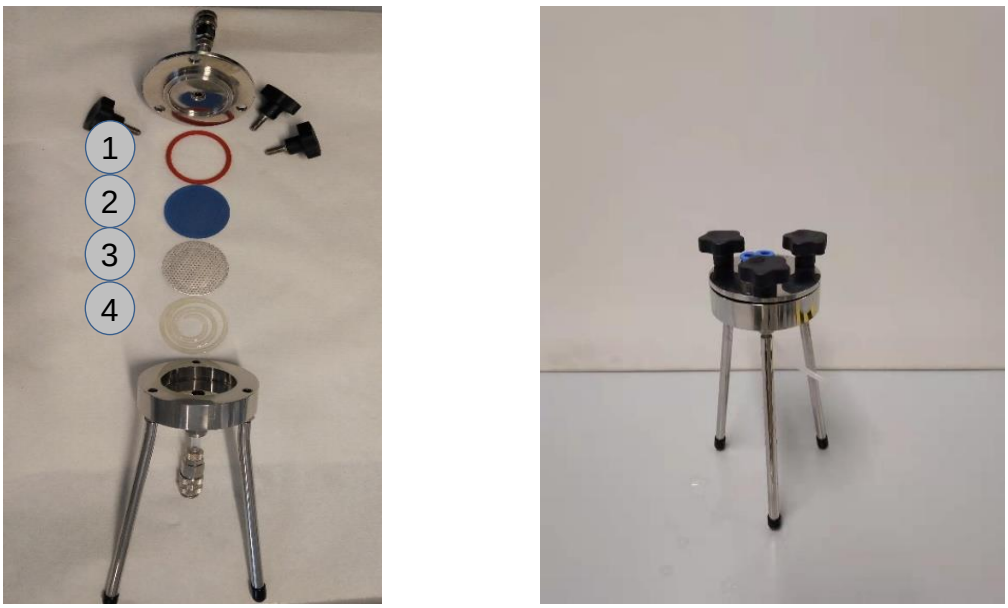

Figure 10: TAMI membrane holder (right) and support layers (left) which are sealing (1), paraffin screen (2), metal screen (3), spiral rubber support (4)

The second bench-scale filtration unit was operated at constant pressure condition (cf. **Figure 11**). The flow rate was determined by weighting the permeate volume at certain time intervals.

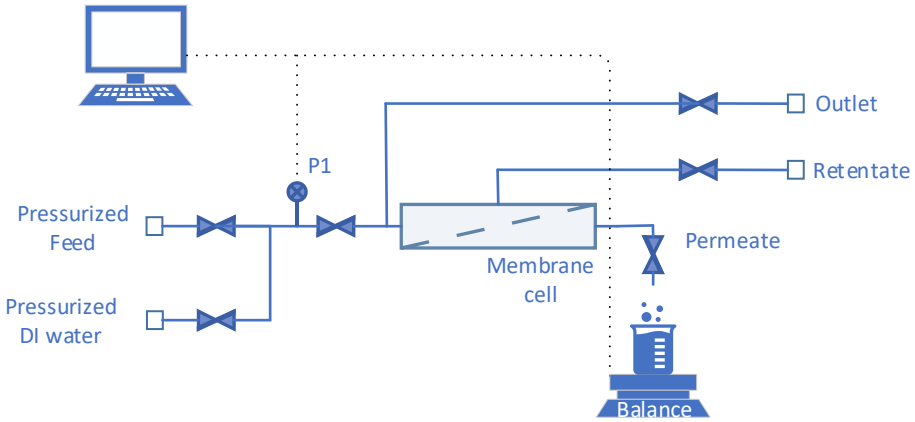

Figure 11: Schematic representation of the bench-scale dead-end filtration unit at constant pressure for flat-sheet membranes

Moreover, one lab-scale filtration unit was implemented within this project. It is designed to test hollow fiber membrane modules at maximum flow rate of about 30 L/h and maximum pressure of 6 bar, cf. **Figure 12**.

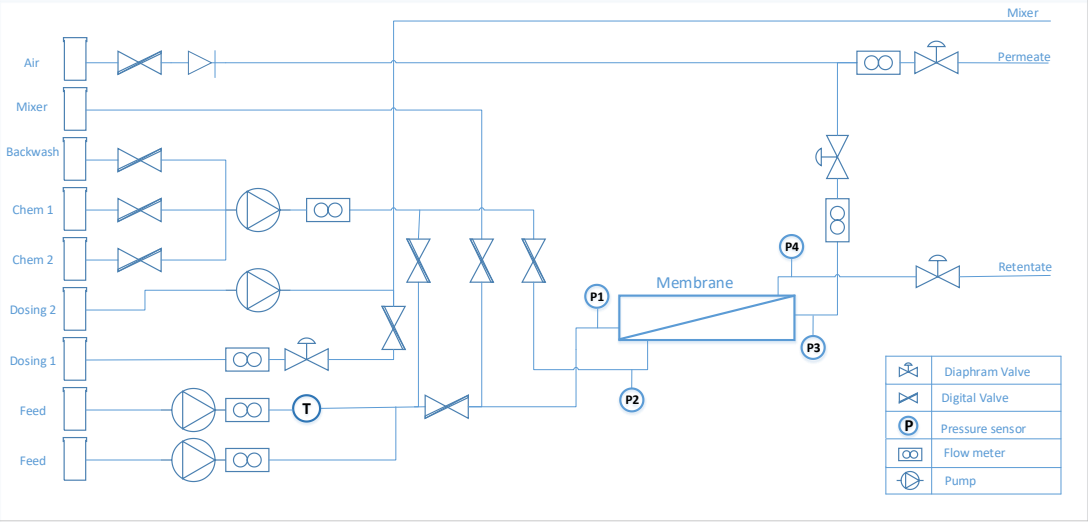

Figure 12: Flowsheet for the lab-scale dead-end filtration unit at constant flow rate for hollow-fiber membranes

3.1.4.2 Filtration experiments with flat sheet membranes

As part of the of the W-UFO II project, more than 150 filtration experiments (about 20% more than planned in the proposal) were performed with FS membranes to gain a detailed understanding of the effects of surfactants and co-surfactants in the model feed emulsions on UF membrane performance, as well as of the potential interactions between surfactants and PES-FS membranes. Two Charges of the UP150 P were tested within the project. Interestingly, membranes of the first charge exhibited initial pure water permeability of about 1,140 L/(m²·h·bar) with a standard deviation of 100 L/(m²·h·bar), second charge indicated a permeability of around 600 L/(m²·h·bar) with a standard deviation of about 190 L/(m²·h·bar). The tested UB50 membranes exhibited a higher deviation in the initial pure water permeability. Various feeds compositions were tested, in which different types and concentrations of surfactants, with and without co-surfactant and salts, were investigated at two oil concentrations of 5 and 10 mg/L. Most of these experiments were carried using UP150 P membranes under constant flux (CF) or pressure (CP) conditions. **Table 4** lists the experiments that were carried out with UP150 P flat sheet membranes and the respective experiment conditions.

All filtration experiments were performed using a virgin membrane. Prior to filtration, FS membranes were cleaned with 50% ethanol solution overnight to eliminate manufacturing residuals and conservatives, and were rinsed with pure water overnight to remove the ethanol. Then, pure water filtration at constant pressure of 1 bar for 30 min were performed as pre-compaction.

Bench-scale one-cycle filtration experiments (i.e., without performing mechanical / chemical cleaning after filtration) were performed at room temperature (~22 C). Dead-end constant flux filtration experiments were conducted at a constant flux of 240 L/(m²·h); the change in transmembrane pressure (TMP), due to fouling, was measured at different time intervals. While dead-end constant pressure filtration experiments were conducted at 0.4 bar, accordingly, the change in membrane flux, due to fouling, was measured at different time intervals. In both filtration modes, a constant volume (300 L/m²) of model feed water was filtered.

Table 4: List of filtration experiments for Nadir® UP150 P flat-sheet membranes using different oil-in-water nano-emulsions at constant flux of 240 L/(m²·h)

Exp. No.	Oil concentration (mg/L)	Surfactant concentration (CMC)			Co-surfactant	Salt
		SDS	Tween20	CTAB		
1	10					
2	-	0.2				
3	-	0.5				
4	-	1				
5	-		0.2			
6	-		0.5			
7	-		1			
8	-			0.2		
9	-			0.5		
10	-			1		
11	-	0.2			X	
12		1			X	
13	-		0.2		X	
14			1		X	
15	-			0.2	X	
16	-	0.2				X
17		1				X
18	-		0.2			X
19			1			X
20	-			0.2		X
21	10	0.2				
22	10	0.5				
23	10	1				
24	10		0.2			
25	10		0.5			
26	10		1			
27	10			0.2		
28	10			0.5		
29	10			1		
30	10	0.2			X	
31	10	1			X	
32	10		0.2		X	
33	10		1		X	
34	10			0.2	X	
35	10	0.2				X
36	10	1				X
37	10		0.2			X
38	10		1			X
39	10			0.2		X

3.1.4.3 Filtration experiments with hollow fiber membranes

Prior to lab-scale filtration experiments, HF membrane modules were rinsed to remove manufacturing residuals, bio-growth inhibitors and conservatives, and soaked overnight with NaOCl (50 ppm). Thereafter, membranes were subjected to a sequence of 1, 2, 3, and 6 h of flushing using DI water at a high flux of 500 L/(m²·h) followed by a relaxation time of 20 min after each filtration period to reduce the membrane compaction influence as well as to ensure complete membrane cleaning. Before every oil nano-emulsion filtration test, initial pure water permeability was determined by filtering DI water until stable membrane permeability was maintained for at least one hour at 100 L/(m²·h).

Multiple-cycle filtration experiments were started with filtering pure water for 15 min, to double check membrane permeability as measured before, then pure water was directly replaced by model oily feed water (i.e., oil nano-emulsion). The membrane filtration testing was lasted for six filtration cycles. Each cycle comprises filtration of oily feed for 45 min at a flux of 100 L/(m²·h) followed by backwashing step at a flux of 230 L/(m²·h) for 60 sec. After the last filtration cycle, pure water permeability was measured again by filtering pure water for 45 min at 100 L/(m²·h) flux, during which backwashing step was made every 15 min at a flux of 240 L/(m²·h) for 60 sec. Thereafter, pure water was filtered through the membrane for 5 min at a flux of 100 L/(m²·h) to define the pure water permeability after each cycle. Finally, membrane cleaning was performed, in which two cleaning steps were carried out in form of cleaning in place, first with SDS at concentration of 0.5 CMC followed by flushing with pure water, then another step of cleaning with NaOCl at concentration of 200 ppm free chlorine was implemented.

3.1.5 Evaluation of membrane fouling

The membrane filtration performance was assessed by determining the filtered volume rate per unit time (Q) and the transmembrane pressure (TMP) along the filtration course, which were then employed to calculate filtration flux (J) and membrane permeability (Pm) at a certain time as following:

$$J\ (L/(m^2 \cdot h)) = \frac{Filtration\ rate}{membrane\ active\ surface\ area} = \frac{Q\ (L/h)}{A_m\ (m^2)} \qquad (1)$$

$$Pm\ (L/(m^2 \cdot \mathrm{h} \cdot \mathrm{bar})) = \frac{J\ (L/(m^2 \cdot h))}{TMP\ (bar)} \quad (2)$$

Subsequently, unitless normalized permeability (NP) during filtration experiment was determined by correlating the membrane permeability ($P_{m,i}$) at a certain filtration point i (one point was registered each 5 sec) to the initial pure water permeability (P_{W0}) measured for every newly fresh membrane prior filtration by filtering DI at the testing conditions (i.e., either constant flux of 240 L/(m²·h) or constant pressure of 0.4 bar), as in equation (3).

$$NP_i = \frac{Pm_i}{P_{W0}} \quad (3)$$

All filtration experiments that were performed at constant flux were repeated 2 – 5 times to investigate the results reproducibility, while filtration experiments performed at constant pressure were carried out one time and only 15 experiments, out of 30, were chosen to be repeated. To evaluate the reproducibility quantitatively, the standard deviation of the normalized permeability for each registered measuring point i (σ_i) was calculated according to equation (4). Thereafter, the average standard deviation of all points was calculated according to equation (5) and referred as “reproducibility indicator”.

$$\sigma_i = \sqrt{\frac{\sum_{j=1}^{j=N}(NP_{i,j} - NP_{i,av})^2}{N_i}} \quad (4)$$

$$\sigma_{tot} = \frac{\sum_{i=1}^{i=n}\sigma_i}{n} \quad (5)$$

whereas N is the number of repetitions for each filtration experiment, n is the number of points in every single experiment.

3.2 Results and discussion

3.2.1 Filtration of model oil feed emulsions using flat sheet membranes

More than 150 filtration experiments (about 20% more than planned in the W-UFO II proposal) were performed using FS membranes to gain better understanding of the effects of surfactants and co-surfactants in the model feed emulsions on UF membrane performance, as well as of the potential interactions between surfactants and PES FS membranes. Various feeds compositions were tested, in which different types and concentrations of surfactants, with and without co-surfactant and salts, were investigated

at the two oil concentrations of 5 and 10 mg/L. Most of these experiments were carried out using UP150 P membranes under constant flux / pressure conditions. **Table 5** lists filtration experiments for UP150 P membranes using complex oil-in-water nano-emulsions (i.e., oil + surfactant) at constant flux, along with the number of trials (N), the average standard deviation of the normalized permeability for each registered measurement point i (according to equation (5)), the average pure water permeability and its respective standard deviation (σ_{Pw0}). The feed composition of each experiment was previously mentioned in **Table 4** in page **13**.

Table 5: List of filtration experiments for Nadir® UP150 P membranes using complex oil-in-water nano-emulsions (i.e., oil + surfactant) at constant flux, along with the number of trials (N), the average standard deviation of the normalized permeability for each registered measurement point, the average pure water permeability and its respective standard deviation

Exp. No.	N	σ_{tot} (-)	P_{w0} (L/(m²·h·bar))	σ_{Pw0} (L/(m²·h·bar))	Exp. No.	N	σ_{tot} (-)	P_{w0} (L/(m²·h·bar))	σ_{Pw0} (L/(m²·h·bar))
1	3	0.045	675	23	**21**	2	0.049	1306	101
2	2	0.024	1365	108	**22**	2	0.033	778	338
3	2	0.007	840	223	**23**	2	0.024	911	237
4	2	0.027	1093	102	**24**	2	0.016	721	236
5	2	0.078	929	238	**25**	3	0.021	982	496
6	2	0.031	1054	249	**26**	2	0.013	806	188
7	2	0.021	1153	145	**27**	3	0.08	968	510
8	2	0.041	908	120	**28**	2	0.013	1276	226
9	2	0.013	985	86	**29**	2	0.106	667	438
10	2	0.008	1014	295	**30**	3	0.115	910	317
11	3	0.083	1048	294	**31**	2	0.032	973	23
12	2	0.05	865	209	**32**	2	0.011	797	411
13	2	0.022	802	217	**33**	2	0.005	1242	73
14	2	0.018	1006	22	**34**	4	0.131	951	345
15	3	0.059	821	345	**35**	3	0.085	893	257
16	3	0.043	770	357	**36**	2	0.005	1196	6
17	2	0.209	1173	24	**37**	2	0.027	532	26
18	2	0.103	759	341	**38**	2	0.012	1012	37
19	2	0.015	948	117	**39**	3	0.154	782	158
20	4	0.213	978	378					

3.2.1.1 Filtration of oil nano-emulsions without additives

Reference experiments were carried out using oil nano-emulsions without additives. **Figure 13** shows the normalized permeability for the reference experiments at

constant flux operation and oil concentration of 10 mg/L. **Figure 13** a shows the filtration curves of three trials and **Figure 13 b** shows the average curve of the three repetitions and the respective graph with min / max error bars. One can already see that some trials were aborted before reaching the 300 L/m² of filtered volume since the feed pressure exceeded the maximum allowed pressure of 3 bar. This also leads to an irregular shape of the average line at the final stage of the experiment (filtered volume V > 200 L/m²). As previously presented in **Table 5**, the average standard deviation σ_{tot} of this experiment was about 0.045, indicating an acceptable reproducibility of the test. Henceforward, to avoid the odd representation of average curves, only one representative filtration curve is presented instead for all upcoming experiments / results along with the respective average standard deviation as indicator to the reproducibility of the experiment.

As indicated in **Figure 13 a** and **b**, a steady decline in the normalized permeability was noticed due to strong membrane fouling in the three trials, such that membrane lost about 90 % of its performance at the end of the filtration experiment. Based on the outputs of W-UFO I, fouling of PES membranes can be explained by combined fouling mechanisms (standard blocking, intermediate blocking, and cake filtration) that are derived by both relation between membrane pore size and oil droplet size distribution as well as hydrophobic -hydrophobic interactions (between oil and the membrane material). Comparing the oil droplet size distribution of nano-emulsions (cf. **Figure 7)** to the MWCO of the membrane (150 kDa, equivalent to barrier pore size < 30 nm) indicates that the membrane should be able to retain oil droplets mainly via surface filtration; however, few small oil droplets can still pass and be retained inside the membrane matrix resulting in the aforementioned combined fouling mechanisms.

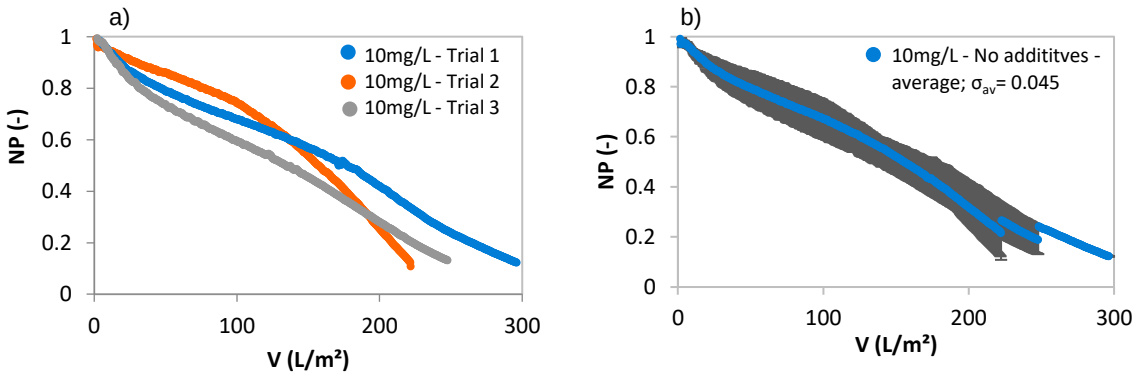

Figure 13: Normalized permeability for UP150 P FS membranes at 10 mg/L oil (without additives) and a flux of 240 L/(m²·h) (a) for three trials (b) as average of the 3 trials with min/max errors

3.2.1.2 Filtration of oil nano-emulsions stabilized by different surfactants

The normalized permeability for three reference filtration tests using surfactants (SDS, Tween 20 and CTAB) solutions, i.e., without oil addition, at concentration of 1 CMC are introduced in **Figure 14 a**. For all surfactants, there was a rapid and sharp decrease in membrane permeability at the beginning of filtration, followed by a plateau. This behavior indicates usually the formation of a rapidly forming pore-blocking layer of surfactant molecules at the membrane surface, followed by the formation of a cake layer with no or very low resistance. However, due to the small size of the surfactants, it is more likely that a large portion of the surfactants will enter the membrane pores and adsorptively accumulate in the supporting structure of the membrane (membrane matrix), which is accompanied by a sharp increase in resistance. After an equilibrium is formed, no further accumulation occurs and the resistance does not increase further. Nevertheless, in other experiments (compare **Figure 14 a, c and e**), it was noticed that reducing the surfactant concentration to 0.5 CMC resulted in a smaller decrease of the membrane permeability, but a plateau was still observed. Decreasing the surfactant concentration to 0.2 CMC led to more consistent decline in membrane performance especially for CTAB and SDS (i.e., indicates no equilibrium or no complete coverage), while Tween 20 showed plateau at all concentrations. These observations support the hypothesis of the adsorptive fouling mechanism with the formation of an equilibrium loading in the matrix as a function of permeate concentration. This adsorptive fouling behavior also has been reported by other researchers, e.g., Trinh et al (2019) (Trinh, Han, Ma, & Chew, 2019).

It can also be seen that the surfactants exhibit analogous fouling, or adsorption behavior, regardless of their different type (i.e., ionic or non-ionic), indicating that adsorption occurs via a hydrophobic-hydrophobic interaction between the relatively hydrophobic PES membrane and the hydrophobic tail of the surfactant molecules. The lower permeability decline in case of Tween 20 compared to SDS and CTAB could be due to its nonionic character, which has a stronger affinity to hydrophobic substances. This finding is quite interesting, specially that it does not match any of the different effects of surfactants on membrane fouling that were introduced in the literature, for instance Trinh et al (2019) reported an increment, no effect and decline in the permeate flux of a microfiltration membranes when filtering CTAB, Tween 20 and SDS, respectively (Trinh et al., 2019). Matos et al (2016) claimed that more fouling was observed in

ceramic membranes when filtering emulsions stabilized with surfactants carrying charges that are opposite to the membrane charge.

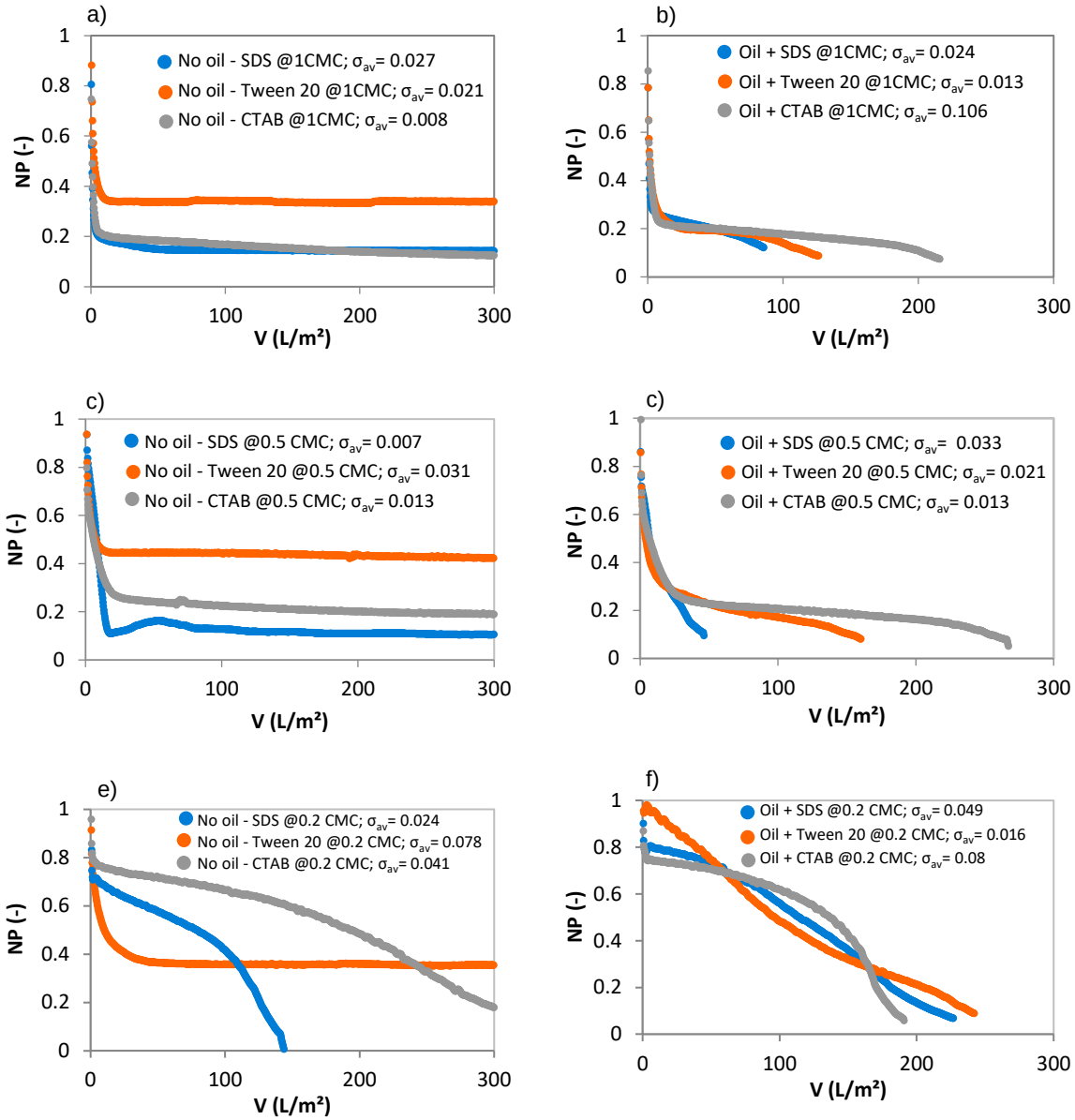

Figure 14: Normalized permeability for UP 150 P at a flux of 240 L/m²·h using surfactants only at concentrations of (a) 1.0, (c) 0.5 and (e) 0.2 CMC as well using oily model emulsions at 10 mg/L oil and surfactants concentration of (b) 1.0, (d) 0.5 and (f) 0.2 CMC

Filtration experiments using oil nano-emulsions containing surfactants showed a fouling behavior that, at least in the early stage, is more comparable to reference experiments using surfactants only rather than reference experiments using oil nano-emulsions without additives. **Figure 14 b** presents the normalized permeability for filtration experiments using complex oil nano-emulsions containing oil at a concentration of 10 mg/L and surfactants at 1 CMC. Although more fouling occurs by the oil as the filtration progresses, as confirmed by the termination of the filtration prior to the filtration

of 300 L/m², this observation indicates that at the employed conditions and the higher surfactant concentration, the fouling was influenced by the surfactants rather than the oil. Moreover, lower surfactant concentrations were found to cause generally lower membrane fouling (compare **Figure 14 b, d and f**). **Figure 14 F** reveals a lower normalized permeability decline at the early stage of filtration compared to the higher surfactant concentrations seen in **Figure 14 b and d.**

Figure 15 presents the normalized permeability for filtration experiments using oil nano-emulsions with the different SDS concentrations of 0.2, 0.5 and 1 CMC, at a fixed oil concentration of 10 mg/L and a constant flux of 240 L/m²·h **(Figure 15 a)** and a constant pressure of 0.4 bar **(Figure 15 b**).

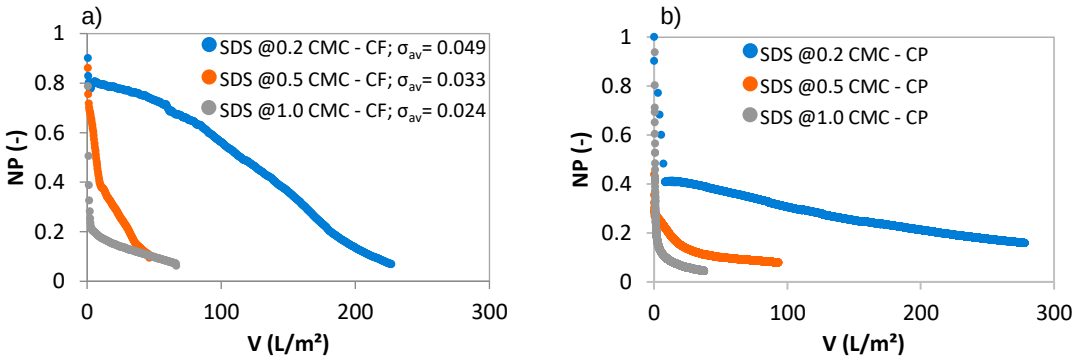

Figure 15: Normalized permeability for UP150 P FS membranes with oil nano-emulsions at 10 mg/L containing SDS at concentrations of 0.2, 0.5 and 1 CMC at (a) constant flux (CF) of 240 L/(m²·h) and (b) constant pressure (CP) of 0.4 bar

Generally, normalized permeability declines for filtration experiments at 0.5 CMC were relatively close to those at 1 CMC. Analogues observations were seen for experiments at constant flux and constant pressure. On the other hand, at constant flux operation, oil nano-emulsions with SDS at 0.2 CMC showed lower permeability decline than in case of 0.5 and 1 CMC, in which, a sharp normalized permeability decline of 20 % was measured at the beginning of the filtration followed by a consistent gradual decline that reached 90% after filtering ~210 L/m². Such permeability decline was measured after filtering less than 50 L/m² in case of 0.5 and 1 CMC. When operating at constant pressure, similar trends were generally observed as in the constant flux experiments. Nevertheless, differences could be observed, especially at an SDS concentration of 0.2 CMC. For instance, a slightly steeper normalized permeability drop in the early filtration phase was observed in the filtration experiments compared to the constant flux operation. Overall, the fouling behavior can be considered comparable for both

operation modes, i.e., constant flux and constant pressure. Especially considering that the experiments of each operation mode were performed with different filtration setups. Thus, the further experiments focused on only constant flux operation because it is more commonly used in practice than constant pressure mode. Moreover, the morphology of fouled UP150 P FS membranes samples were analyzed using scanning electron microscope (SEM) and compared with pristine unfouled membranes**.** As indicated in **Figure 16** SEM micrographs showed no significant alterations in the fouled membranes cross-sections compared to pristine membrane.

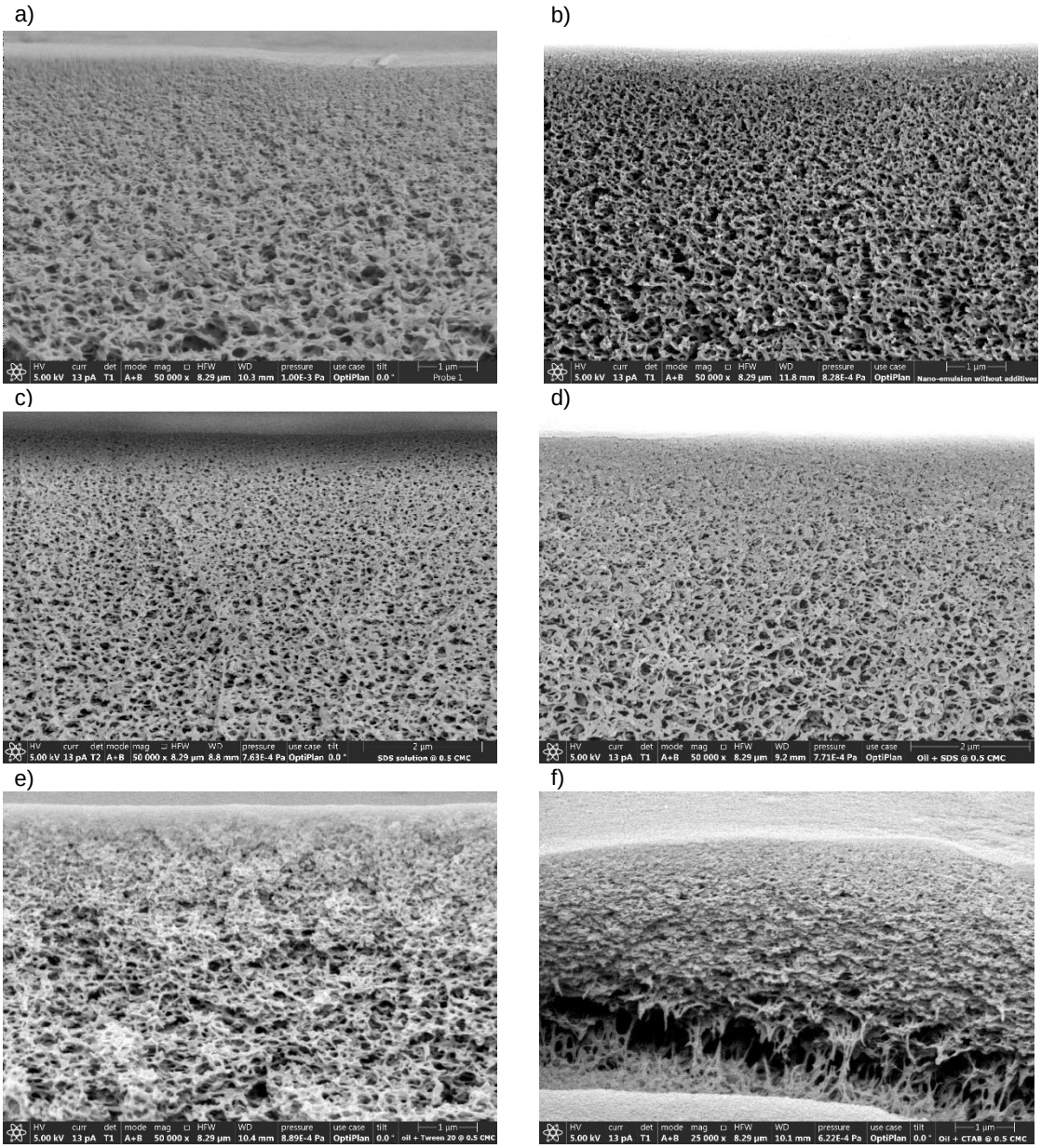

Figure 16: SEM micrographs for the cross-section morphologies of UP150 P membranes, pristine (fresh) membrane (a), in addition to fouled membranes after filtration of oil nano-emulsions without additives (b), SDS solutions at concentrations of 0.5 CMC (c), oil nano-emulsions stabilized by SDS at 0.5 CMC (d), Tween 20 at 0.5 CMC (e) and CTAB at 0.5 CMC (f)

This might indicate no oil penetration to the membrane matrices, i.e., most of membrane fouling (and performance decline) occurred due to surface fouling (oil and/or surfactant adsorption to the membranes surfaces). These observations contradict with earlier claims (cf. section 3.2.1.1) that few small oil droplets might be able to pass into the membrane matrix. Nevertheless, more quantitative analysis to the permeates in different experiments is certainly required to examine / validate these hypotheses. These tasks are planned to be a part of W-UFO III^{+} project.

3.2.1.3 Influence of co-surfactants and salts on the filtration of oil nano-emulsions stabilized by different surfactants

The influences of oil nano-emulsions containing co-surfactant and artificial seawater salts on the FS membranes performance were studied for the three types of surfactants. **Figure 17** shows the normalized permeability for filtration experiments of surfactants solutions at concentration of 0.2 CMC containing 2-pentanol and artificial seawater salts (3.5 g/L), without oil in **Figure 17 a, c and e** and with oil at 10 mg/L in **Figure 17 b, d and f**. In the reference experiments without oil nano-emulsions, a slightly smaller decrease in the normalized permeability was observed with the addition of the co-surfactant (2-pentanol), which was more pronounced for SDS than for the other two surfactants. That might be related to the enhanced solubility of the surfactants in water, and hence, less adsorption on or in the membrane.

Dosing ASW at concentration of 3.5 g/L was found to change the fouling behavior and cause additional fouling in reference experiments in different ways. Less total fouling was noticed in case of SDS and slightly more fouling was noticed in case of Tween 20. Moreover, reference experiments with CTAB and ASW salt were not reproducible. This is due to the fact that CTAB hardly dissolved in water when ASW was added. It is known that salts reduce the solubility of surfactants in water and the CMC (Wan & Poon, 1969). Micelle formation reduces the concentration of free surfactants and thus the equilibrium loading or fouling on or in the membrane. On the other hand, a micelle may well have a size in the range of the small pores of a UF, which can lead to blocking of pores and thus to increased fouling. Corresponding reference experiments with FS and model oil-emulsions with salts but without surfactants were carried out in W-UFO I. The results showed that the dosage of salts was associated with lower membrane fouling, regardless of whether the salts were dosed in form of single salts, e.g., NaCl or $CaCl_2$, or as a mixture e.g. ASW (Idrees et al., 2019). The interaction between SDS and ASW and their influence on the fouling behavior of HF membranes by model oil-

emulsions was also partly studied in previous work. It was observed that both SDS and ASW tend to reduce the membrane fouling. However, the interaction of SDS and ASW caused additional membrane fouling (Idrees et al., 2021).

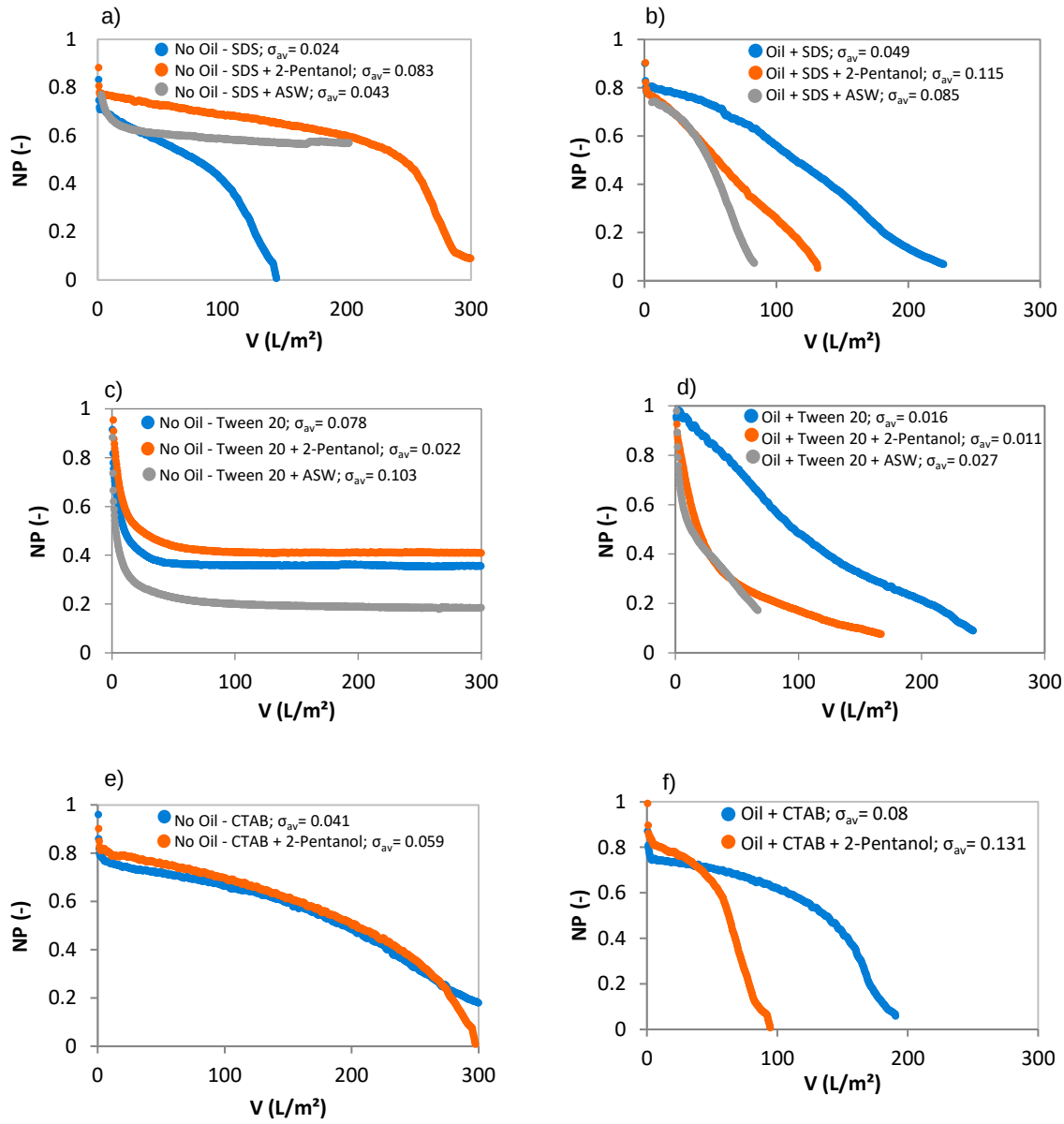

Figure 17: Normalized permeability for UP150 P FS membranes with surfactant, 2-pentanol and ASW at a flux of 240 L/m²·h. On the left side reference experiments without oil using (a) SDS, (c) Tween 20 and (e) CTAB and on the right side those with oil nano-emulsions with 10 mg/L oil and (b) SDS, (d) Tween 20 and (f) CTAB

Overall, one can conclude from bench-scale one-cycle filtration experiments using FS membranes that dosing surfactants, co-surfactant and ASW exacerbate the membrane fouling of oil-emulsions at the employed experimental conditions. Stronger membrane fouling can be mainly interpreted by excessive adsorptive fouling by the surfactants on the membrane surface, and most likely inside internal porous structure because of the

small surfactant molecular sizes (although not demonstrated in SEM analysis to date). Interestingly, when a critical surfactant concentration is exceeded (approx. 0.5 CMC for 10 mg/L oil), the influence of surfactants on fouling already dominates at the beginning of filtration. In the further course of filtration, oil or fouling layer formation gains more and more influence.

It is important to note that no mechanical backwashing was performed in these experiments. Therefore, despite the important findings on the fundamental mechanisms from the studies with a flat sheet membrane, experiments with backwashable hollow fiber membranes are inevitable.

3.2.2 Filtration of model oil feed emulsions using hollow fiber membranes

A set of lab-scale filtration experiments were carried out using hollow fiber (HF) PES membranes to investigate the influences of additives on the membrane performance at conditions close to full-scale application as well as the backwashability (and fouling reversibility) of the membranes after filtering oil nano-emulsions stabilized by surfactants. Generally, membranes showed an average initial pure water permeability of P_{W0} = ~700 L/(m²·h·bar) with a standard deviation of 140 L/(m²·h·bar). Also, the experiments showed better reproducibility than those with FS membranes as will be introduced in details in the following sections.

3.2.2.1 Filtration of oil nano-emulsions without additives

At the beginning, reference tests using oil-emulsions without additives, were carried out at oil concentrations of 5, 10 and 25 mg/L and a constant flux of 100 L/(m²·h). Experiments with 5 mg/L were conducted five times, of which two were performed for three cycles, one with four cycles and two with six cycles. **Figure 18** shows the average normalized permeability in which a steady decline of the permeability was found such that the membranes lost about 50% of their initial performance after three filtration cycles, and more than 60% after six filtration cycles. The reference experiments impressively showed that hydraulic backwash was not able to sufficiently restore the initial membrane permeability; in some experiments it restored only about 5%, while in the best case it barely reached 10%.

Two trials of reference experiments with 10 mg/L oil-emulsions, without additives (**Figure 19**) suffered a permeability decline of about 20, 40 and 70 - 80% of the initial permeability at the end of the 1st, 2nd and 6th cycle, respectively.

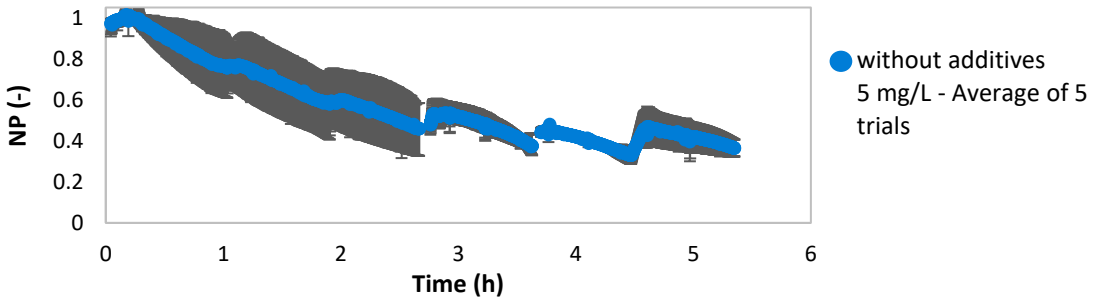

Figure 18: Normalized permeability for reference filtration tests using oil nano-emulsions without additives at a concentration of 5 mg/L employing PES-HF membranes at a constant flux of 100 L/(m²·h), 5 trials with min/max error bars

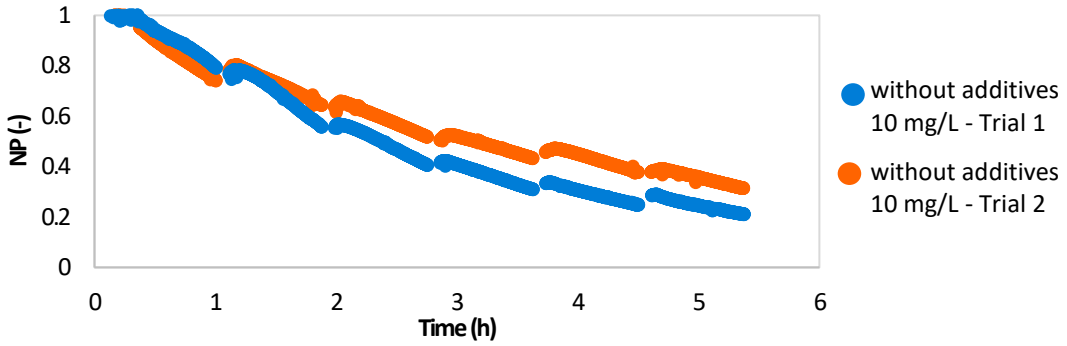

Figure 19: Normalized permeability for reference filtration tests using oil nano-emulsions without additives at aconcentration of 10 mg/L employing PES-HF membranes at a constant flux of 100 L/(m²·h) for 6 filtration cycles, 2 trials

Furthermore, as shown in **Figure 20**, a sharp decrease in permeability was observed in the reference experiments with 25 mg/L oil-emulsions without additives, which was about 80 and 85 % of the initial permeability at the end of the first and second cycles, respectively. However, in the next cycles the permeability was stable at this low level. At the end of the sixth cycle, a permeability decrease of 90 % was measured.

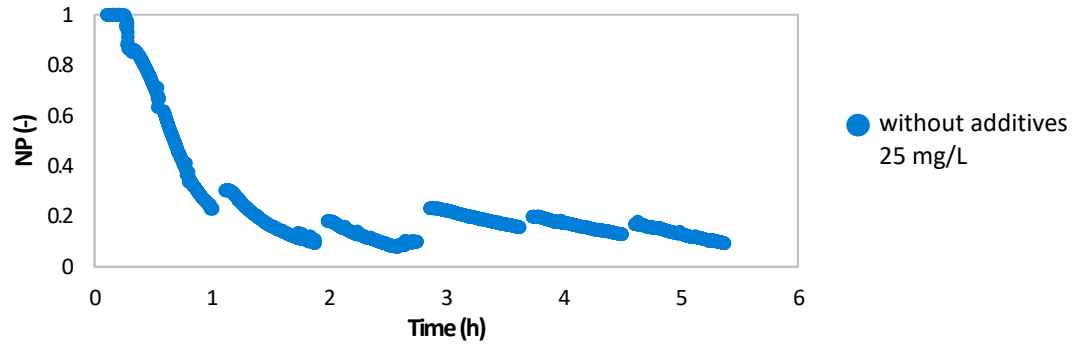

Figure 20: Normalized permeability for reference filtration tests using oil nano-emulsions without additives at a concentration of 25 mg/L employing PES-HF membranes at a constant flux of 100 L/(m²·h) for 6 filtration cycles, 1 trial

For comparison, the normalized permeability for representative reference filtration experiments without additives are presented in **Figure 21**. Generally, more performance decay within the filtration cycle was seen with increasing oil concentration. As aforementioned in section 3.2.1, fouling of PES-UF membranes by oil-contaminated feeds was related to a pore blocking fouling mechanism. In no case was it possible to restore the initial membrane permeability by hydraulic backwashing with deionized water. In contrast, backwashing with the conventional backwashing parameters hardly shows any effectiveness. The hydrophobic-hydrophobic interaction forces between oil and membrane are obviously too strong.

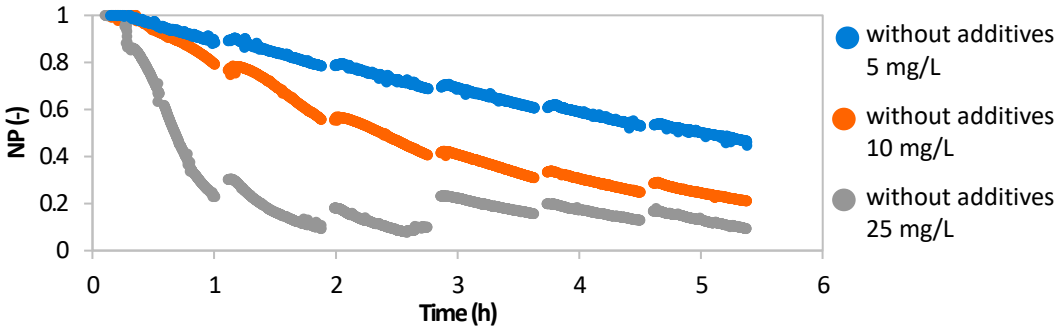

Figure 21: Normalized permeability for reference filtration tests using oil nanoemulsions without additives employing PES-HF membranes at a constant flux of 100 L/(m²·h) for 6 filtration cycles

3.2.2.2 Filtration of SDS solutions without oil

Multiple cycles reference filtration experiments were carried out with SDS at concentrations of 0.01, 0.05, 0.1, 0.2 and 0.5 CMC without oil, and at a constant flux of 100 L/(m²·h). SDS concentration of 0.1 CMC showed an initial permeability decline of about 18%, as depicted in **Figure 22**. Thereafter, the permeability was stable till the next backwash step, in which the initial membrane permeability was completely restored. The following filtration cycles showed almost the same pattern as the first cycle. Since SDS is believed to be dissolved in water at the applied conditions, it cannot be retained by the membrane. Subsequently, it is assumed that the initial permeability decline is either caused by adsorption of SDS in the internal porous structure of the PES-HF membrane. Once the adsorption equilibrium or the maximum load of the filter is reached, one can expect that no further SDS would be adsorbed or attached onto the membrane, which might explain the noticed plateau after certain filtration time.

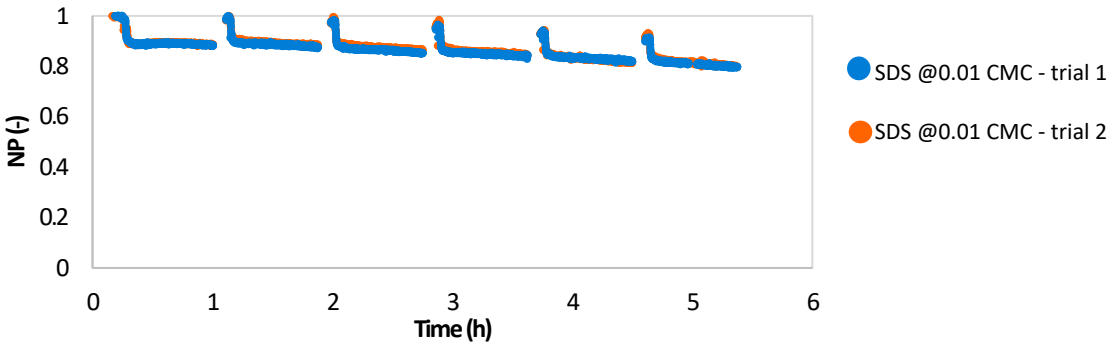

Figure 22: Normalized permeability for reference filtration tests using SDS solutions at a concentration of 0.01 CMC employing PES-HF membranes at a constant flux of 100 L/(m²·h) for 6 filtration cycles, 2 trials

In addition, as indicated in Figure 25**Figure 23,** multiple cycles reference tests using SDS at a concentration of 0.2 CMC showed a comparable permeability decline pattern to the case of 0.1 CMC, reaching a permeability decline of ~20% at the end of all filtration cycles. Also, the hydraulic backwash was able to completely restore the initial membrane performance.

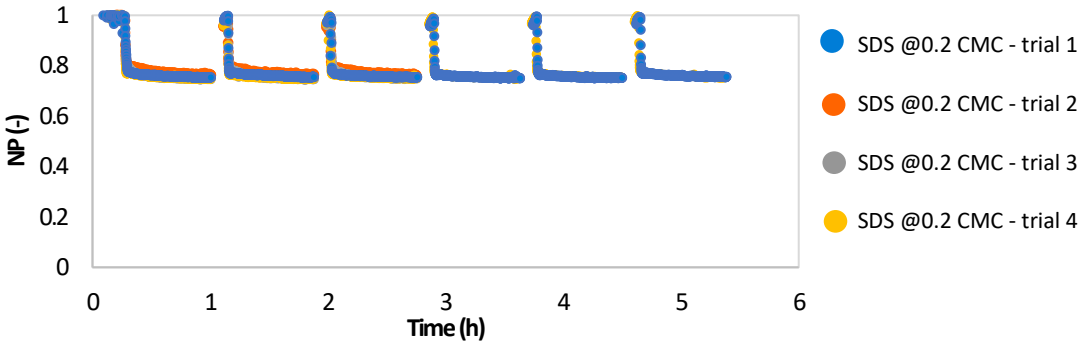

Figure 23: Normalized permeability for reference filtration tests using SDS solutions at a concentration of 0.2 CMC employing PES-HF membranes at a constant flux of 100 L/(m²·h), 4 trials.

Multiple cycles reference tests using SDS at 0.5 CMC (**Figure 24**) showed a sharp permeability decline at the beginning of every filtration cycle, in which the membrane lost more than 80% of its performance followed by a short plateau. This stronger initial decrease indicates that more SDS is bound to the membrane surface / matrix than in case of lower SDS concentrations. Nevertheless, the hydraulic backwash was able to completely restore the initial membrane performance, as in case of lower SDS concentrations.

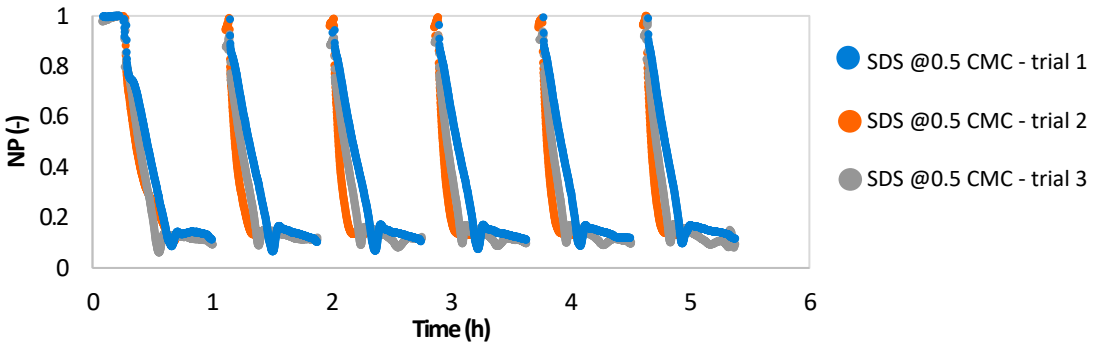

Figure 24: Normalized permeability for reference filtration tests using SDS solutions at a concentration of 0.5 CMC employing PES-HF membranes at a constant flux of 100 L/(m²·h) for 6 filtration cycles, 3 trials

For comparison, **Figure 25** shows the representative normalized permeability for reference multiple cycles filtration experiments with SDS solutions at different concentrations of 0.01, 0.05, 0.2 and 0.5 CMC. Reference filtration using SDS at concentrations of 0.01, 0.05 and 0.2 CMC exhibited limited normalized permeability decline of ~10%, 18 and 20%, respectively, at the beginning of the first cycle followed by a plateau.

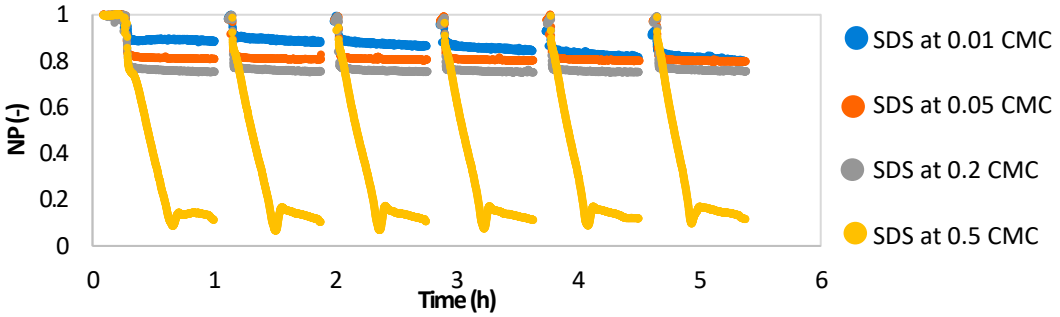

Figure 25: Normalized permeability for reference filtration tests using SDS solutions at different concentrations of 0.01, 0.05, 0.2 and 0.5 CMC employing PES-HF membranes at a constant flux of 100 L/(m²·h) for 6 filtration cycles

This is consistent with the observed performance in the filtration tests using FS membranes (cf. **Section 3.2.1** and **Figure 14**). As the low molecular weight SDS cannot be retained by a sieving effect from the membrane under the given conditions, the initial sharp decrease in permeability can be interpreted by the adsorption of SDS in the inner porous structure of the membrane (i.e. the membrane matrix). Once adsorption equilibrium is reached, no more SDS adsorbs and a plateau is formed. Surprisingly, the initial membrane permeability could be fully restored by simple hydraulic backwashing. The interaction forces between the anionic surfactant and the membrane are obviously minimal. All further filtration cycles (up to the sixth cycle) showed almost the same pattern as the first cycle. There was no formation of irreversible fouling.

3.2.2.3 Filtration of oil nano-emulsions stabilized by SDS

Oil nano-emulsions containing 5 and 10 mg/L oil and SDS at different concentrations of 0.01, 0.05, 0.1, 0.2 and 0.5 CMC were filtered through HF membranes at a constant flux of 100 L/(m²·h). Filtration experiments of nano-emulsions with an oil concentration of 5 mg/L stabilized by SDS at different concentrations of 0.01, 0.05 and 0.1 CMC are depicted in **Figure 26 a, b and c**, respectively. Experiments using oil nano-emulsions containing SDS at 0.01 CMC (cf. **Figure 26 a)** exhibited a total performance decay of ~ 20 % compared to ~ 60 % in case of reference filtration of oil nano-emulsions with 5 mg/L without additive. A comparable fouling behavior was observed for other oil nano-emulsions with SDS content up to 0.1 CMC, which can be seen in **Figure 26 b and c**.

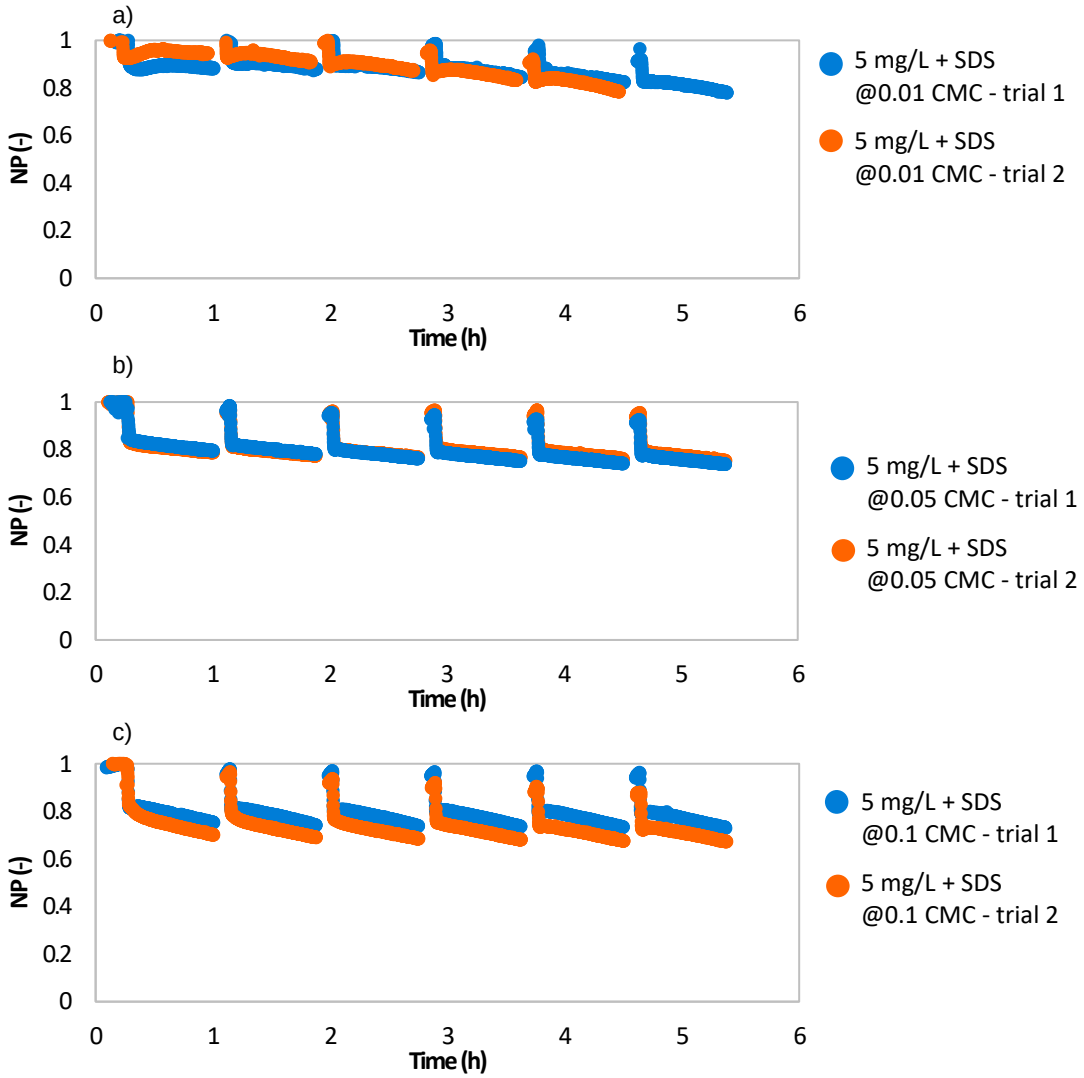

Figure 26: Normalized permeability for filtration experiments using oil nano-emulsions containing 5 mg/L oil and SDS at different concentrations of (a) 0.01, (b) 0.05 and (c) 0.1 CMC employing PES-HF membranes at a constant flux of 100 L/(m²·h)

As can be seen in **Figure 27 a and b**, increasing the SDS concentration to 0.2 and 0.5 CMC, respectively, resulted in a greater decrease in normalized permeability, which reached about 90 % in the case of SDS at 0.5 CMC. This implies the dominant impact(s) of SDS in membrane fouling as well as the adsorptive fouling mechanism. On the other hand, interestingly, hydraulic backwashing at the end of each cycle actually restored more than 95 % of the initial membrane performance.

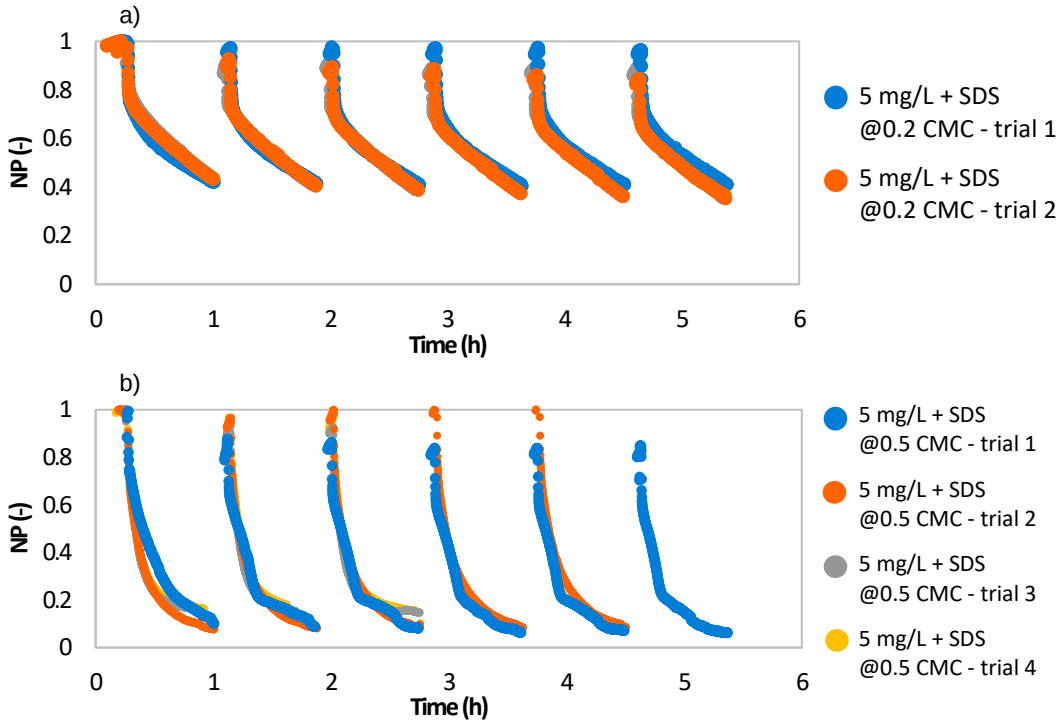

Figure 27: Normalized permeability for filtration experiments using oil nano-emulsions containing 5 mg/L oil and SDS at different concentrations of (a) 0.2 and (b) 0.5 CMC employing PES-HF membranes at a constant flux of 100 L/(m²·h)

Comparing the filtration curves for oil nano-emulsions containing 5 mg/L oil and SDS at different concentrations of 0.01, 0.05, 0.1, 0.2 and 0.5 CMC, cf. in **Figure 28,** it can be seen that the permeability decline is more comparable to the corresponding decline in the reference experiments with SDS without oil than to that in the experiments with model oil-emulsions without additives. This was indeed already observed in the experiments with FS membranes.

Accordingly, the fouling mechanisms also by HF membranes are most likely prevailed by the adsorption of surfactant (SDS) to the membrane matrix. This remarkable improvement in the backwashability of the deposited oil droplets from the membrane by dosing SDS can be attributed, on the one hand, to the formation of an intermediate layer of SDS between the oil and the membrane. This layer and with it the retained oil

can then be removed comparatively easily by backwashing. On the other hand, the dosage of surfactants could lead to an improvement of the mixing between oil and water by reducing the interfacial energy, which could also increase the backwashing efficiency. A combined effect of both mechanisms may also occur.

A comparable fouling behavior was observed for other model oil-emulsions with up to 0.1 CMC of SDS, although an increasing SDS concentration led to a stronger decrease of the normalized permeability (in the case of SDS at 0.5 CMC about 90 %). This shows the dominant influence of SDS on membrane fouling under these conditions. On the other hand, even with these model oil-emulsions, more than 95% of the initial permeability could be restored by hydraulic backwashing at the end of each cycle.

This effect, found in the research project, opens up the possibility of controllable irreversible fouling, which could potentially enable the filtration of such oil concentrations in dead-end operation, which so far can only be treated in cross-flow with very high overflow velocities.

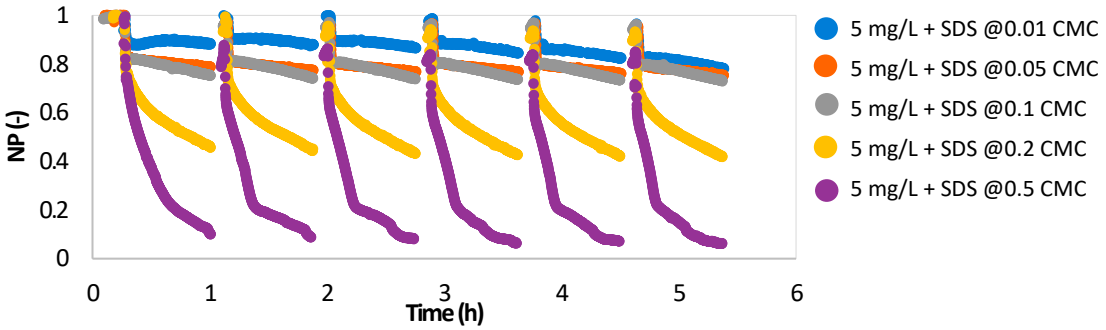

Figure 28: Normalized permeability for filtration experiments using oil nano-emulsions containing 5 mg/L oil and SDS at different concentrations of 0.01, 0.05, 0.1, 0.2 and 0.5 CMC employing PES-HF membranes at a constant flux of 100 L/(m²·h) for 6 filtration cycles

Subsequently, further filtration experiments were conducted using oil nano-emulsions at the higher oil concentrations of 10, 25, and 50 mg/L. Filtration experiments with oil nano-emulsions at an oil concentration of 10 mg/L and the low SDS concentration of 0.01 CMC (see **Figure 29**) revealed that SDS caused additional fouling within the filtration cycles without significant enhancement in the fouling reversibility, such that, the experiment was aborted during the third cycle. This is because strong performance decay was measured in the first cycle (50%) and hydraulic backwashing was not able to restore the initial membrane permeability (severe irreversible fouling via hydrophobic-hydrophobic interaction). Subsequently, the feed pressure during the 3rd cycle

exceeded the maximum allowed pressure of 4 bar (due to severe fouling) and the test was automatically aborted.

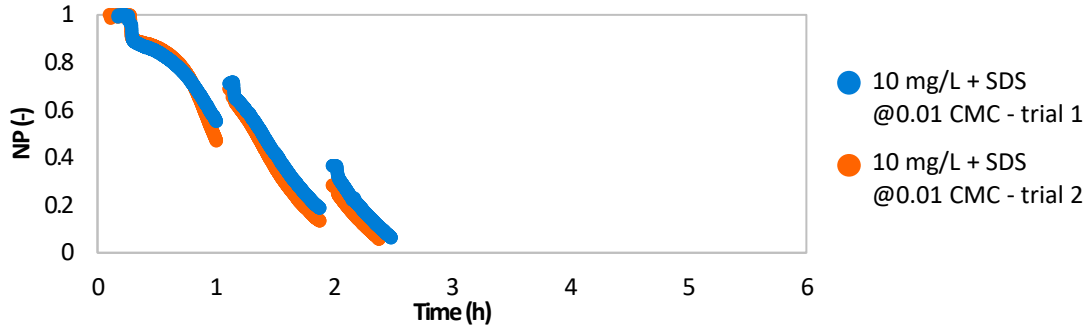

Figure 29: Normalized permeability for filtration experiments using oil nano-emulsions containing 10 mg/L oil and SDS at concentration of 0.01 CMC employing PES-HF membranes at constant flux of 100 L/(m²·h)

Increasing the SDS concentration to 0.05 and 0.1 CMC, as presented in **Figure 30 a** and **b**, respectively, also resulted in additional fouling within the filtration cycles, but was sufficient to achieve predominantly reversible fouling. For instance, only about 20 and 25% irreversible fouling was measured at the beginning of the 6th cycle when 0.05 and 0.1 CMC were dosed, respectively.

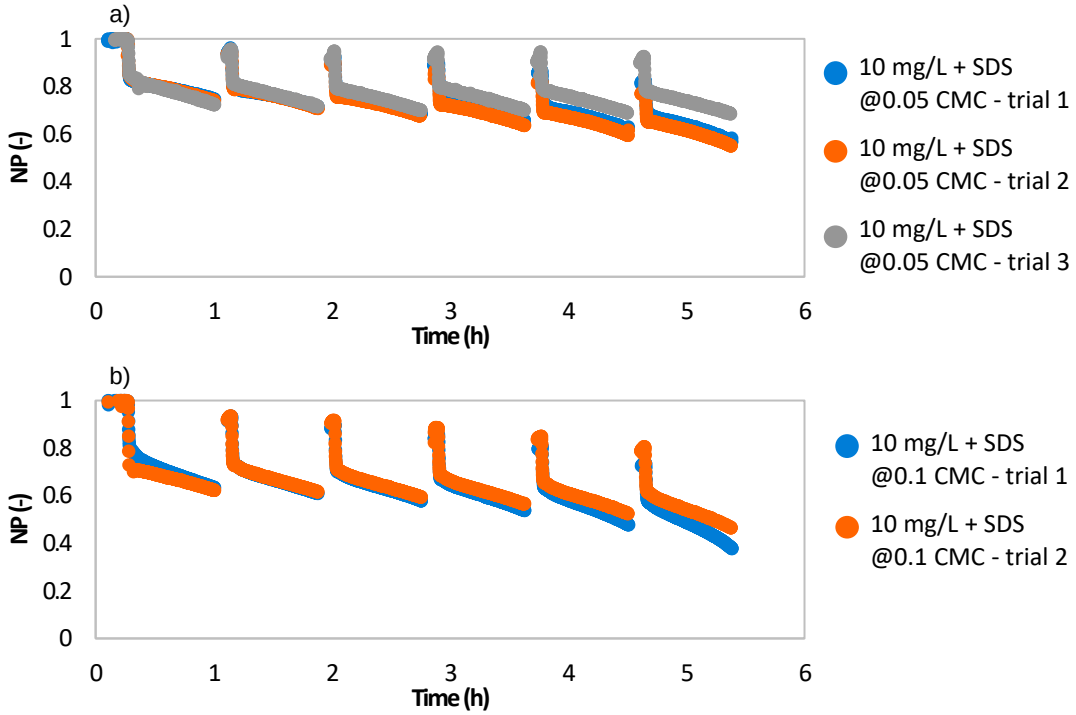

Figure 30: Normalized permeability for filtration experiments using oil nano-emulsions containing 10 mg/L and SDS at different concentrations of (a) 0.05 and (b) 0.1 CMC employing PES-HF membranes at a constant flux of 100 L/(m²·h) for 6 filtration cycles

Further increment in the SDS concentration resulted in a sharp decline in the permeability within the cycle. For example, the membranes lost about 50 and 90% of their permeability at the end of the first cycle when filtering oil nano-emulsions with 10 mg/L oil and SDS concentration of 0.2 and 0.5 CMC, respectively (cf. **Figure 31**). For instance, oil nano-emulsion with SDS at 0.5 CMC showed performance decay of 80% within the first cycle that increased to 90% at the 6th cycle. Nevertheless, the reversible fouling contribution was still dominant as well such that hydraulic backwashing could restore 80% of the initial permeability implying that the membrane suffered from only ~ 20% irreversible fouling.

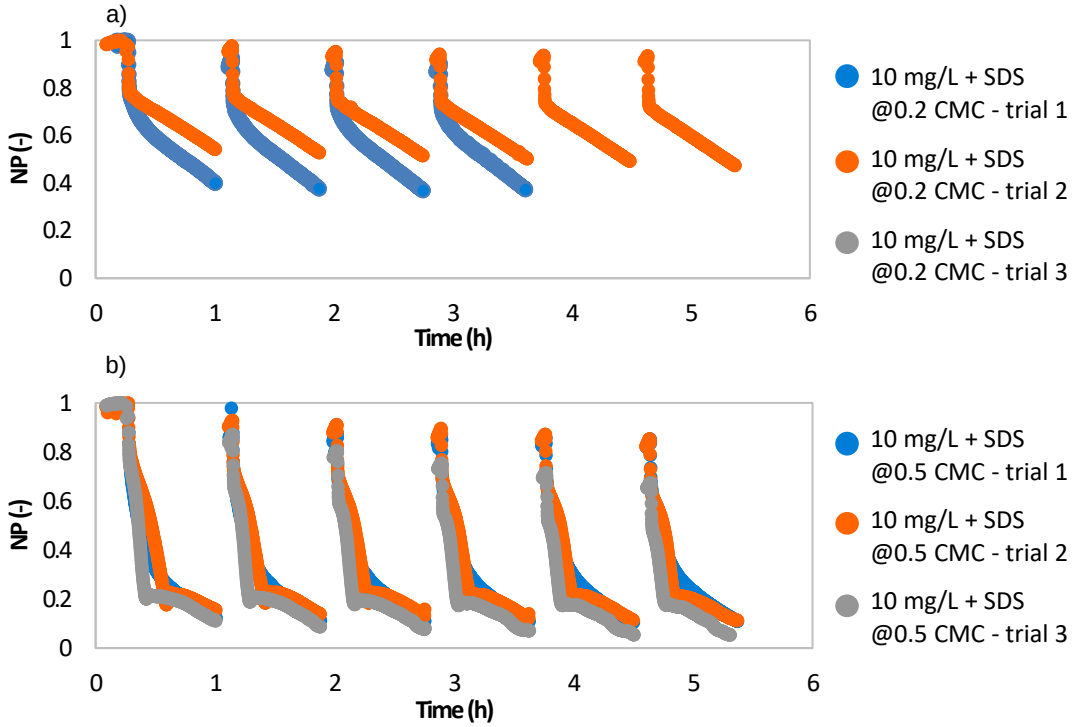

Figure 31: Normalized permeability for filtration experiments using oil nano-emulsions containing 10 mg/L and SDS at different concentrations of (a) 0.2 and (b) 0.5 CMC employing PES-HF membranes at a constant flux of 100 L/(m²·h)

Figure 32 compares the representative normalized permeability declines curves for the aforementioned lab-scale filtration tests using oil nano-emulsions with 10 mg/L oil content. The addition of SDS at concentrations in the range of 0.05 – 0.5 CMC could generally promote the fouling reversibility, whereas addition of SDS at 0.01 CMC was found to be insufficient such that the filtration experiment was aborted after three cycles only. This shows that there is a critical ratio between SDS and oil concentration which must be exceeded to obtain the desired effect. Increasing the SDS concentrations led to improved reversibility. However, with increasing SDS concentrations, fouling by SDS

also increased. Within the experimental conditions and the set concentrations, the dosage of 0.2 CMC SDS was optimal.

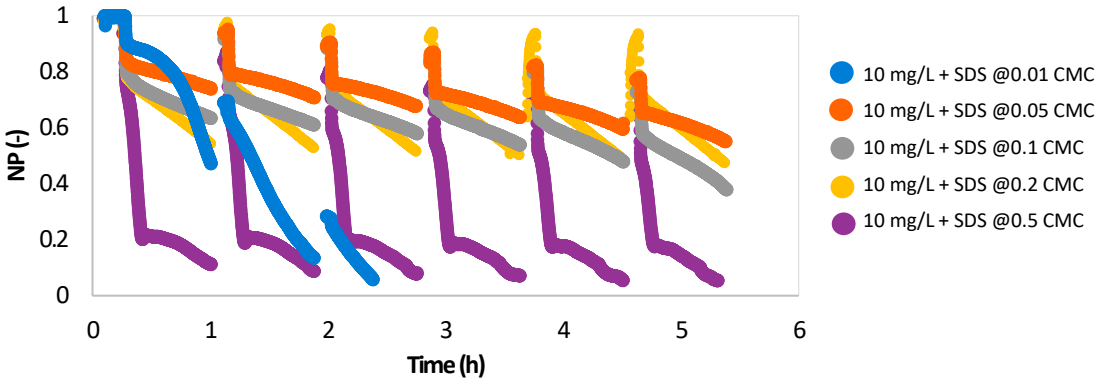

Figure 32: Normalized permeability for filtration experiments using oil nano-emulsions containing 10 mg/L and SDS at different concentrations of 0.01, 0.05, 0.1, 0.2 and 0.5 CMC employing PES-HF membranes at a constant flux of 100 L/(m²·h).

Furthermore, multiple cycles lab-scale filtration experiments were performed at the higher oil concentrations of 25 and 50 mg/L, at constant SDS concentration of 0.2 CMC and a constant flux of 100 L/(m²·h). The results are plotted in **Figure 33** and **Figure 34**, respectively. Increasing the oil concentration resulted in the higher performance decrease of 40 - 75 % and ~80 % within the first cycle for 25 and 50 mg/L, respectively. Even though more membrane fouling was indeed expected at higher oil concentrations, the measured performance decay was much less than predicted. Irreversible fouling of only about 22 % and 28 % were determined after five cycles for filtration experiments at oil concentrations of 25 and 50 mg/L, respectively. It is worth noting that such good membrane performance at such high oil concentration at dead-end operation has not been reported in the literature before.

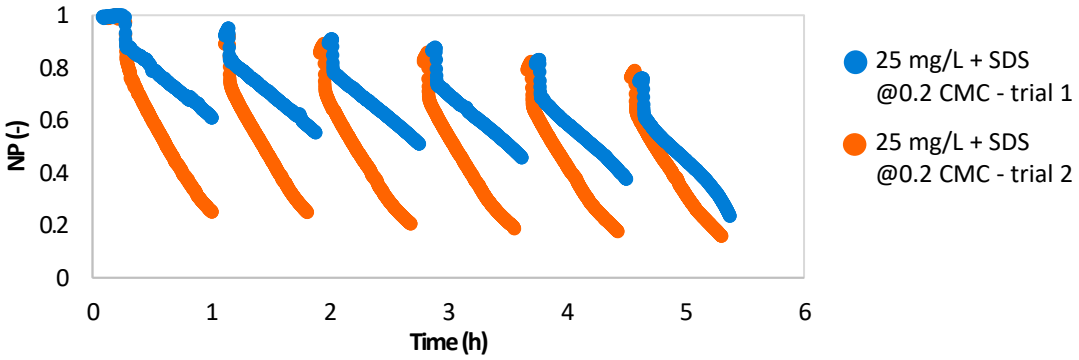

Figure 33: Normalized permeability for filtration experiments using oil nano-emulsions containing 25 mg/L and SDS at concentration of 0.2 CMC employing PES-HF membranes at a constant flux of 100 L/(m²·h), 2 trials

Nevertheless, filtration experiments with oil nano-emulsions with 50 mg/L oil and 0.2 CMC of SDS were not successful in all the trials performed. As presented in **Figure 34**, the second and third trials were automatically aborted, during the first filtration cycle, as feed pressure exceeded the 4 bar limit. This breakdown can be counteracted with a high degree of certainty by adjusting the operating conditions (e.g. shortening the duration of the filtration cycle). Among other things, this is the subject of the investigations of the follow-up project W-UFO III^{+}.

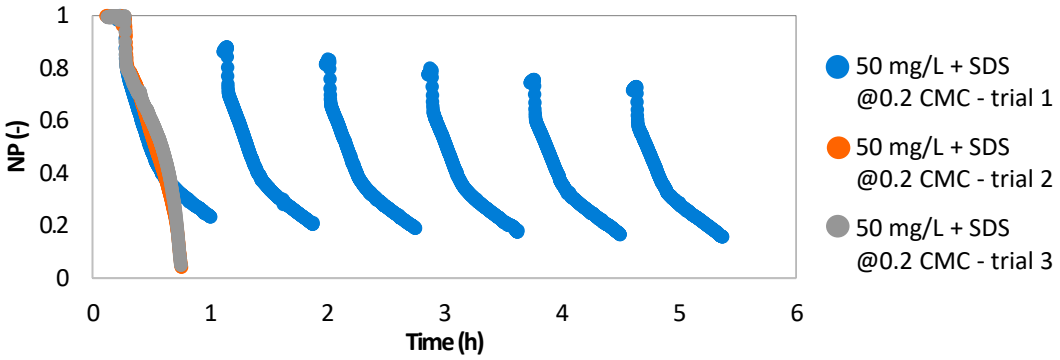

Figure 34: Normalized permeability for filtration experiments using oil nano-emulsions containing 50 mg/L oil and SDS at concentration of 0.2 CMC employing PES-HF membranes at a constant flux of 100 L/(m²·h), 3 trials

3.2.2.4 Filtration of oil nano-emulsions stabilized by Tween 20

Lab-scale filtration experiments prior to multiple filtration cycle experiments for testing the backwashability and the cleanability of HF membranes fouled by oil nano-emulsions containing Tween 20 were carried out. These experiments were conducted at oil concentration of 5 mg/L and Tween 20 concentrations of 0.2 and 0.5 CMC at a constant flux of 100 L/(m²·h). Significant irreversible membrane fouling was noticed at both Tween 20 concentrations. **Figure 35** shows a significant drop of more than 60 % of the initial permeability, which could be restored by a maximum of 15 % by hydraulic backwashing. Such strong irreversible fouling can be attributed to the non-ionic character of Tween 20, which caused too strong hydrophobic-hydrophobic interaction between the elongated lyophilic (non-ionic) tail in Tween 20 and the relatively hydrophobic membrane material. As a result, it was decided not to include Tween 20 in the lab-scale filtration experiments, and instead more attention was paid to the promising results obtained by adding SDS.

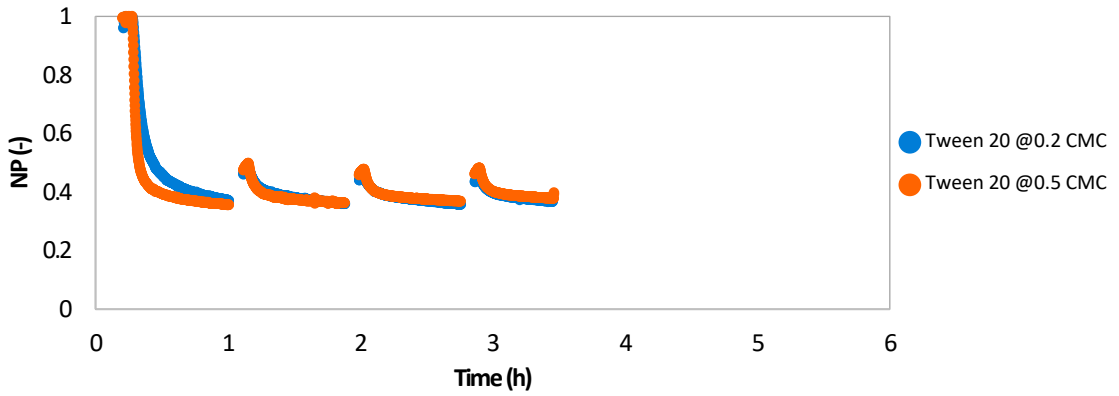

Figure 35: Normalized permeability for filtration of 5 mg/L oil nano-emulsions containing Tween20 at concentrations of 0.2 and 0.5 CMC employing PES-HF membranes at a constant flux of 100 L/(m²·h)

3.2.2.5 Separation performance during the filtration of oil nano-emulsions stabilized by SDS

In parallel, the separation performance during lab-scale filtration experiments with SDS were analyzed. **Figure 36** introduces the TOC retention values during filtration tests using oil nano-emulsions at oil concentrations of 5, 10 and 25 mg/L and SDS concentrations of 0, 0.05, 0.1, 0.2 and 0.5 CMC. Generally, it was revealed that the higher the oil concentration in feed, the higher TOC retention was measured. TOC retentions of 87%, 95% and 97% were determined for the reference experiments without additives at oil contents of 5, 10, and 25 mg/L, respectively. Despite of its very positive impact on the fouling propensity, addition of SDS was found to significantly decrease the TOC retention, whereby the membrane retention decreased by increasing SDS dosage. SDS is not retained by the membrane and thus increases the TOC concentration in the permeate. The associated disadvantages will be further investigated in the follow-up project W-UFO III^{+}.

To confirm that the oil can be mostly retained by the UF membrane also by SDS dosing, and SDS is the main reason for the high TOC values in the permeate, feed and permeate from the filtration experiments using oil nano-emulsions containing 10 mg/L oil and at the different SDS concentrations of 0, 0.05, 0.2 and 0.5 CMC were further analyzed with respect to dissolved oil fractions, polycyclic aromatic hydrocarbons (PAH). The concentrations of the 16 main types of PAH, according to the US-EPA, were determined.

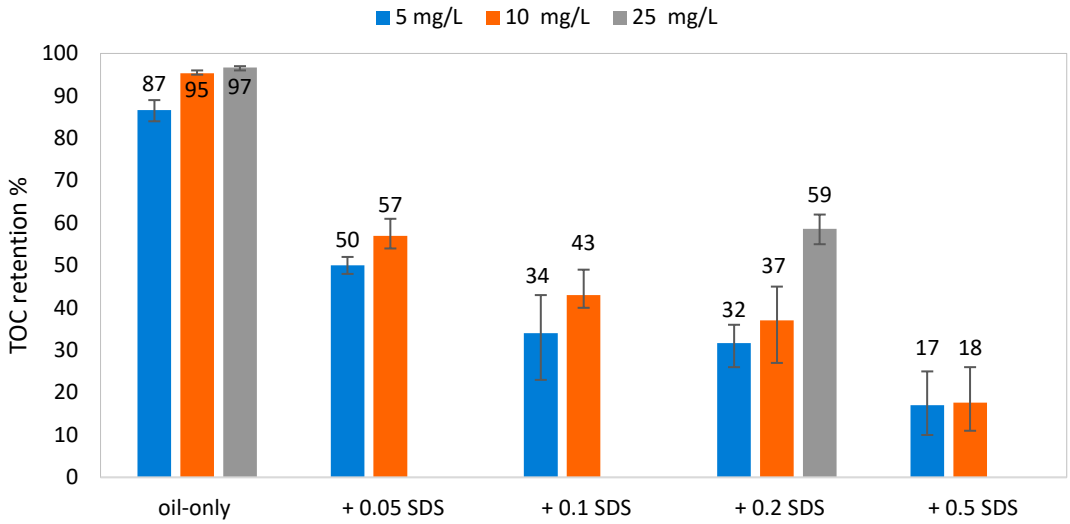

Figure 36: TOC retention of PES-HF membranes for model oil-emulsions with different oil and SDS concentrations at a constant flux of 100 L/m²·h·bar. The presented values are the average of three samples collected at the beginning and the end of 1st cycle and at the beginning of 2nd cycle

Figure 37 shows 11 types of PAH that could be found in the model oil-emulsion without SDS in concentrations higher the limit of determination. **Figure 38** shows the calculated retention of the respective PAHs by PES-HF membranes. Except for acenaphthylene and fluoranthem, no significant variation in membrane retention due to different SDS dosages was observed for any of the PAH compounds. This indicates that the dosing of SDS does not lead to a higher passage of oil components, but that the increase in TOC is only due to the passage of SDS through the membrane.

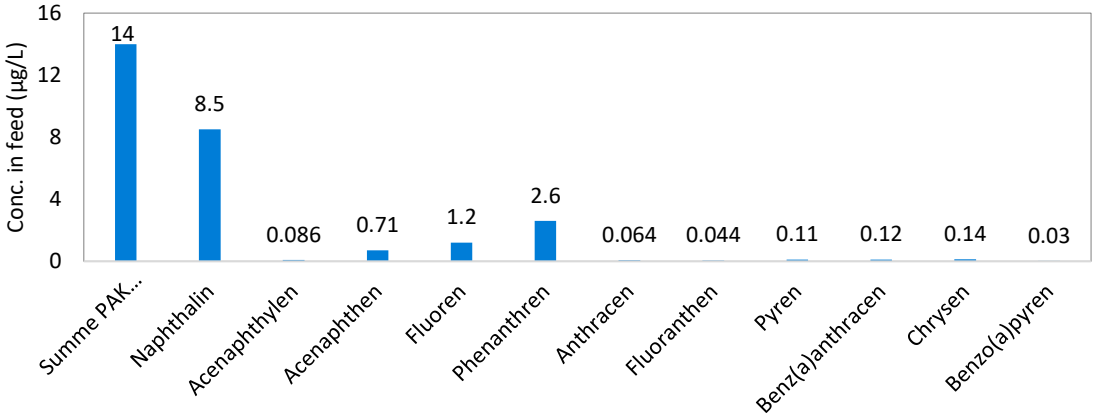

Figure 37: Concentration of 11 types of polycyclic aromatic hydrocarbons existing in the model oil-emulsion at 10 mg/L oil (as TOC) and without SDS

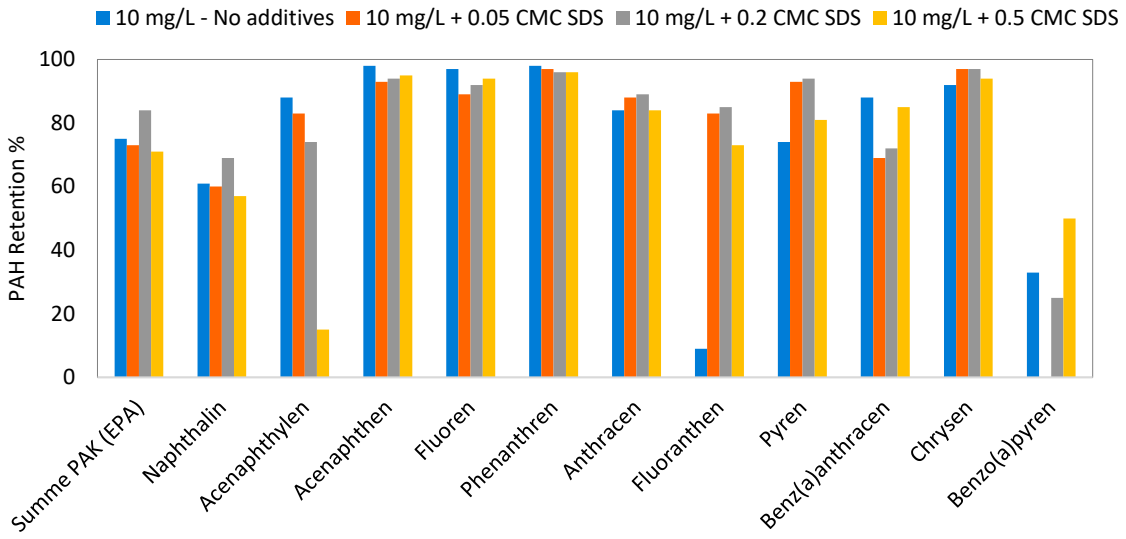

Figure 38: Retention of 11 types of polycyclic aromatic hydrocarbons in the model oil-emulsions containing 10 mg/L oil (as TOC) and various concentrations of SDS

3.3 Conclusion and outlook

The W-UFO II subproject investigated the effects of using surfactants and co-surfactants as well as salts on

- oil nano-emulsion stability,
- dead-end UF membrane performance, and
- the fundamental fouling mechanisms

using

- flat sheet membranes in single-cycle filtration and
- backwashable hollow fiber membranes in multiple cycles.

Overall, it can be concluded from the experiments with flat sheet membranes that the dosage of surfactants, co-surfactants and salts increase the membrane fouling of oil-emulsions under the experimental conditions used. The stronger membrane fouling probably due to adsorptive fouling by the surfactants on the membrane surface and most likely within the inner porous structure due to the small molecular sizes of the surfactants. Interestingly, when a critical surfactant concentration is exceeded (in this study about 0.5 CMC for 10 mg/L oil), there is a dominant influence of the surfactants on the fouling right at the beginning of the filtration. In the further course of filtration, the oil or the fouling layer formation gains more and more influence.

The same observation could be made in the experiments with hollow fiber membranes. Surprisingly, in the experiments with SDS, the initial membrane permeability could be completely restored by simple hydraulic backwashing. The interaction forces between

the anionic surfactant and the membrane are obviously only small. All further filtration cycles (up to the sixth cycle) showed almost the same pattern as the first cycle. No irreversible fouling was formed. This effect could not be demonstrated with the non-ionic surfactant Tween 20. Here, strong irreversible fouling occurred.

The considerable improvement in the backwashability of the deposited oil droplets from the membrane through the dosing of SDS can be attributed on the one hand to the formation of an intermediate layer of SDS between the oil and the membrane. This layer and with it the retained oil can then be removed comparatively easily by back-washing. Secondly, the dosage of surfactants could lead to an improvement of the mixing between oil and water by reducing the interfacial energy, which could also in-crease the backwashing efficiency. A combined effect of both mechanisms may also occur.

It was shown that there is a critical ratio between SDS and oil concentrations that must be exceeded to gain the desired effect. Increasing SDS concentrations above this value results in improved fouling reversibility. However, as the SDS concentrations increases, the fouling due to SDS also increases, so there is an upper limit here as well. Results to date indicate that dead-end operation is possible with SDS dosing even for oily wastewaters with higher oil concentrations (up to at least 50 mg/L).

This effect, found in the research project, opens up the possibility of controllable irre-versible fouling, which could potentially enable the filtration of such oil concentrations in dead-end operation, which so far can only be treated in cross-flow with very high overflow velocities.

The improvement in backwashability and reduction in irreversible fouling by dosing SDS for dead-end operation of the UF hollow fiber membrane is even stronger than the effect obtained by surface modification of the same membrane using a zwitterionic hydrogel coating, as reported in Idrees et al. (2021) (Idrees et al., 2021). As shown in Figure 39, irreversible fouling of about 50% was observed for the surface-modified membrane when filtering a model oil-emulsion containing 1 mg/L oil (without additives) after 16 filtration cycles, compared to about 80% in the case of the unmodified standard membrane. In addition, filtration of model oil-emulsions with oil concentrations higher than 5 mg/L was not possible. This indicates that although the surface modification was able to improve the antifouling properties, it cannot be extended to large-scale

applications, since a significant part of the membrane fouling is still irreversible and filtration of feed with higher oil concentrations is not possible.

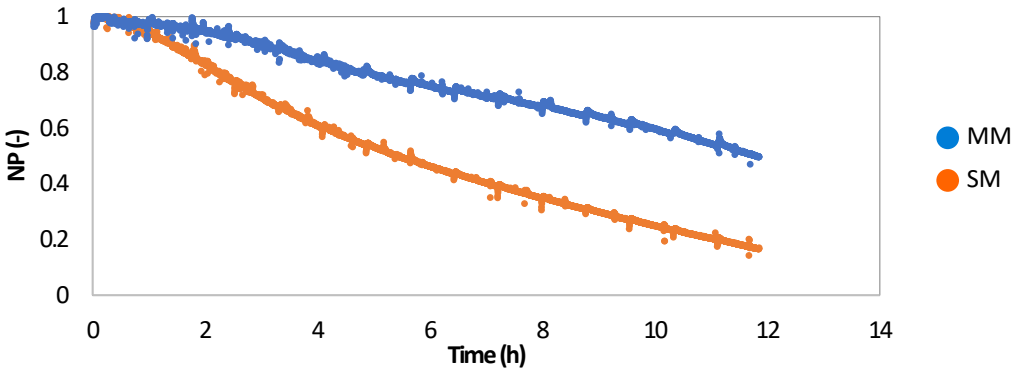

Figure 39: Normalized permeability for filtering 1 mg/L oil nano-emulsions without additives through HF standard UF membrane (SM) and surface modified membrane (MM) at a constant flux of 100 L/(m²·h) for 16 cycles

The next phase of the project, **W-UFO III⁺**, will combine all knowledge and expertise gained through W-UFO I and W-UFO II to achieve the following objectives:

- Studying the impact of SDS dosing method on the membrane performance and the permeate quality, and investigation of the most-suited dosing conditions, which allow using reduced SDS amounts without compromising the overall treatment process efficiency.
- Quantitative determination of dissolved oil fractions in the model feed water and permeate water, besides proper understanding of their impact(s) on membrane fouling behavior and SDS mechanisms of action.
- Investigating the feasibility of synergistic combination of UF technology and other separation techniques (i.e., powdered activated carbon (PAC) and coagulation) for improving the permeate quality and, possibly, the membrane performance.
- Optimization of the main influencing operating parameters, as revealed from W-UFO I and W-UFO II (i.e., SDS dosing method, filtration flux, filtration cycle duration, backwashing flux, and duration, post pure water filtration).
- Studying the potential environmental impact(s) of SDS dosing and identifying the tolerable SDS concentration ranges in the permeate depending on its further use, in addition to investigating the most reliable applications for water reuse.
- Validating the applicability of the developed treatment protocol / procedure for other compositions of OWWE (reflecting other produced water sites).

- Performing sustainability and cost assessment to evaluate the reliability of the new treatment protocol via comparing the investment and operating costs of SDS-enhanced UF dead-end filtration with the so far preferred crossflow membrane filtration.

4 References

Funk, W., Dammann, V., & Donnevert, G. (2005). *Qualitätssicherung in der analytischen chemie: anwendungen in der umwelt-, lebensmittel-und werkstoffanalytik, biotechnologie und medizintechnik*: John Wiley & Sons.

Idrees, H., ElSherbiny, I., & Panglisch, S. (2019). *“Weitergehende Untersuchungen zum Fouling von Ultrafiltrationsmembranen bei der Aufbereitung von ölhaltigen Wässern” (W-UFO I)*. Retrieved from https://willy-hager-stiftung.de/forschungsfoerderung/gefoerderte-vorhaben

Idrees, H., ElSherbiny, I. M. A., Hecket, M., Ke, Q., Staaks, C., Khalil, A. S. G., . . . Panglisch, S. (2021). Surface Modification of Ready-to-Use Hollow Fiber Ultrafiltration Modules for Oil/Water Separation. *Chemie Ingenieur Technik, 93*(9), 1408-1416. doi:https://doi.org/10.1002/cite.202100044

Trinh, T. A., Han, Q., Ma, Y., & Chew, J. W. (2019). Microfiltration of oil-emulsions stabilized by different surfactants. *Journal of Membrane Science, 579*, 199-209. doi:https://doi.org/10.1016/j.memsci.2019.02.068

Wan, L. S. C., & Poon, P. K. C. (1969). Effect of salts on the surface/interfacial tension and critical micelle concentration of surfactants. *Journal of Pharmaceutical Sciences, 58*(12), 1562-1567. doi:https://doi.org/10.1002/jps.2600581238

5 Appendix

Table A 1: List of filtration experiments for Nadir® UP150 P FS membranes using different oil-in-water nano-emulsions at a constant flux (CF) of 240 L/(m²·h) and constant pressure (CP) of 0.4 bar.

Exp. No.	Filtration mode	Oil concentration (mg/L)	Surfactant concentration (CMC)			Co-surfactant	Salt
			SDS	Tween20	CTAB		
1	CF	10					
2	CF	-	0.2				
3	CF	-	0.5				
4	CF	-	1				
5	CF	-		0.2			
6	CF	-		0.5			
7	CF	-		1			
8	CF	-			0.2		
9	CF	-			0.5		
10	CF	-			1		
11	CF	-	0.2			x	
12	CF		1			X	
13	CF	-		0.2		X	
14	CF			1		X	
15	CF	-			0.2	X	
16	CF	-	0.2				X
17	CF		1				X
18	CF	-		0.2			X
19	CF			1			X
20	CF	-			0.2		X
21	CF	10	0.2				
22	CF	10	0.5				
23	CF	10	1				
24	CF	10		0.2			
25	CF	10		0.5			
26	CF	10		1			
27	CF	10			0.2		
28	CF	10			0.5		
29	CF	10			1		
30	CF	10	0.2			X	
31	CF	10	1			X	
32	CF	10		0.2		X	
33	CF	10		1		X	
34	CF	10			0.2	X	
35	CF	10	0.2				X
36	CF	10	1				X
37	CF	10		0.2			X
38	CF	10		1			X

Exp. No.	Filtration mode	Oil concentration (mg/L)	Surfactant concentration (CMC)			Co-surfactant	Salt
			SDS	Tween20	CTAB		
39	CF	10			0.2		X
41	CP	10					
42	CP	-	0.2				
43	CP	-	0.5				
44	CP	-	1				
45	CP	-		0.2			
46	CP	-		0.5			
47	CP	-		1			
48	CP	-			0.2		
49	CP	-			0.5		
50	CP	-			1		
51	CP	-	0.2			X	
52	CP	-		0.2		X	
53	CP	-			0.2	X	
55	CP	-		0.2			X
56	CP	-			0.2		X
57	CP	10	0.2				
58	CP	10	0.5				
59	CP	10	1				
60	CP	10		0.2			
61	CP	10		0.5			
62	CP	10		1			
64	CP	10			0.5		
65	CP	10			1		
66	CP	10	0.2			X	
67	CP	10		0.2		X	
68	CP	10			0.2	X	
70	CP	10		0.2			X
71	CP	10			0.2		X

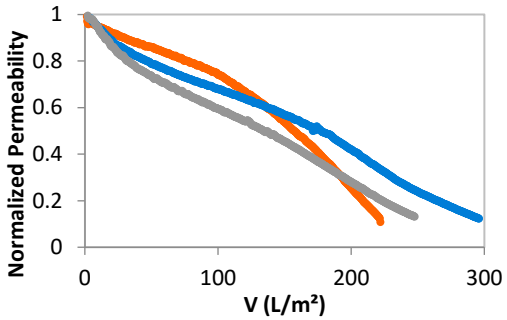

Figure A 1: Experiment No. 1

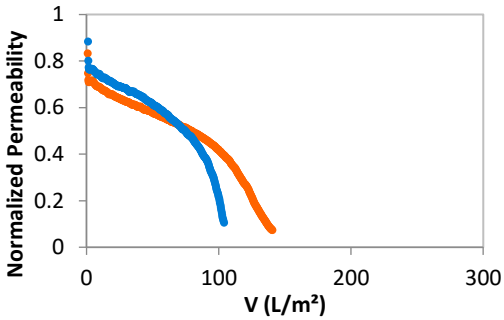

Figure A 2: Experiment No. 2

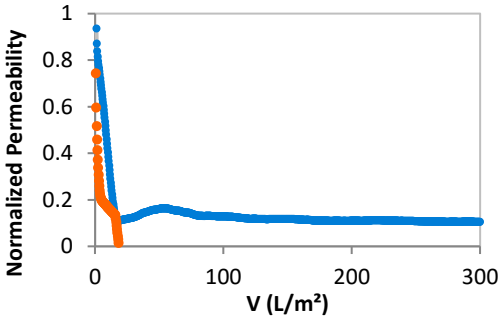

Figure A 3: Experiment No. 3

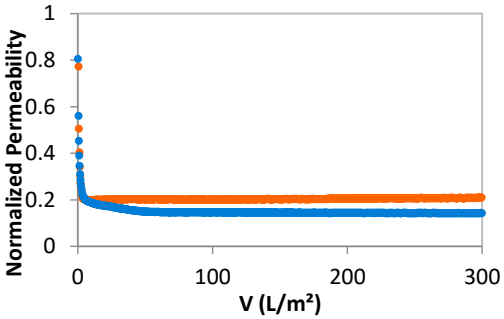

Figure A 4: Experiment No. 4

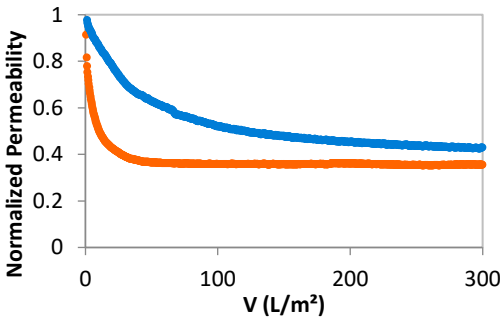

Figure A 5: Experiment No. 5

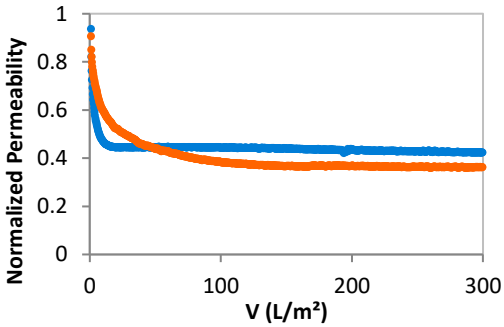

Figure A 6: Experiment No. 6

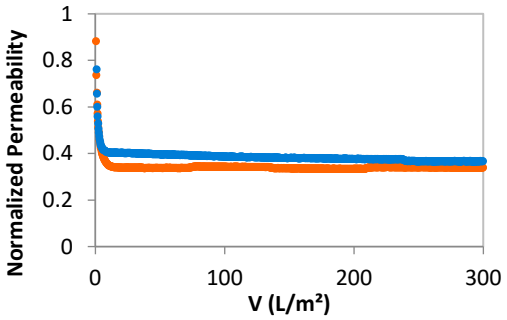

Figure A 7: Experiment No. 7

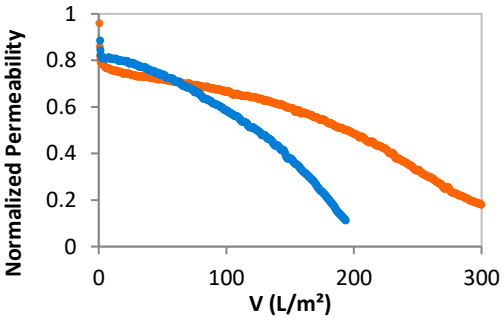

Figure A 8: Experiment No. 8

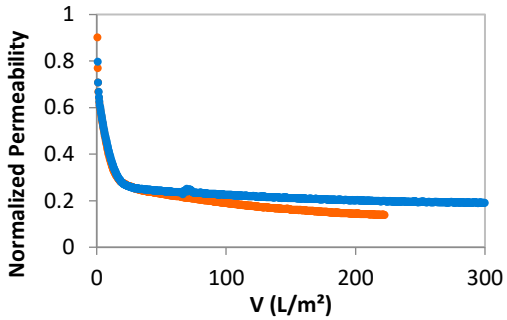

Figure A 9: Experiment No. 9

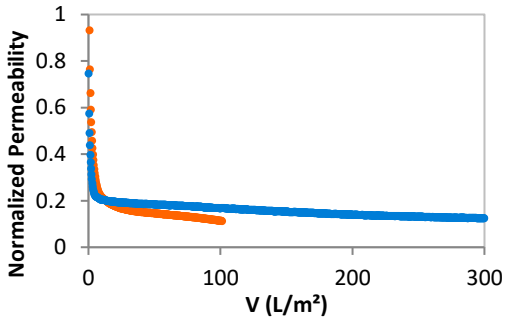

Figure A 10: Experiment No. 10

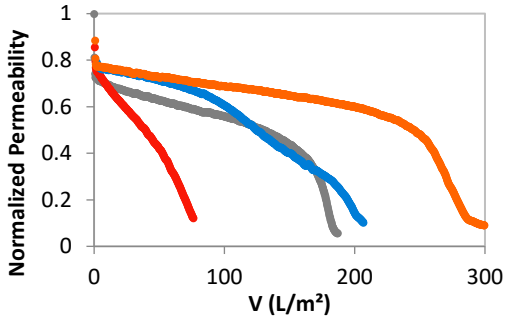

Figure A 11: Experiment No. 11

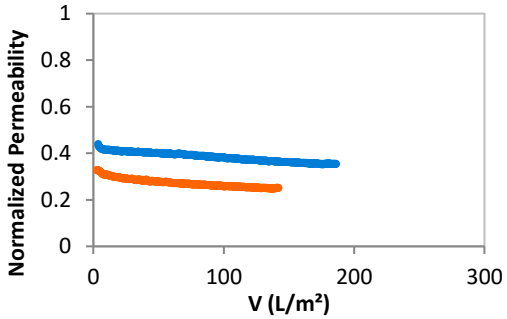

Figure A 12: Experiment No. 12

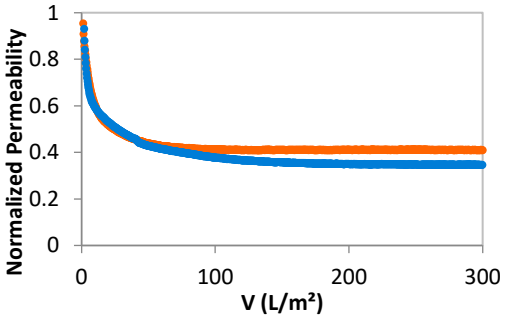

Figure A 13: Experiment No. 13

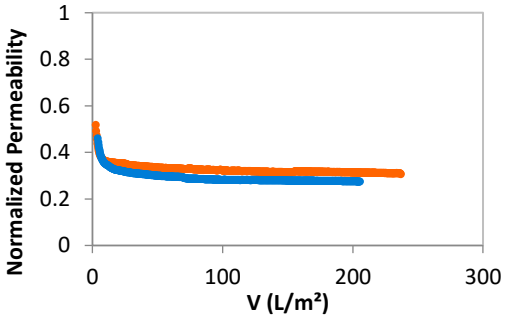

Figure A 14: Experiment No. 14

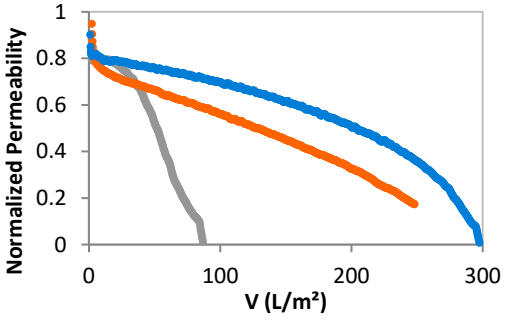

Figure A 15: Experiment No. 15

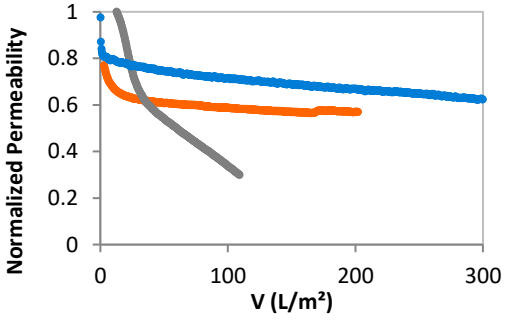

Figure A 16: Experiment No. 16

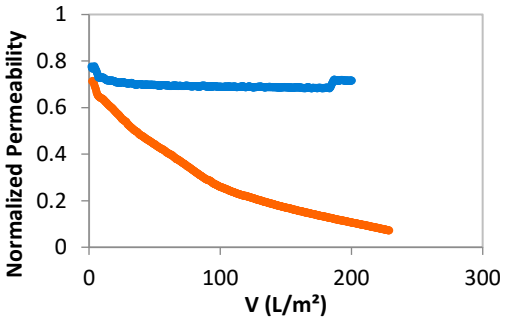

Figure A 17: Experiment No. 17

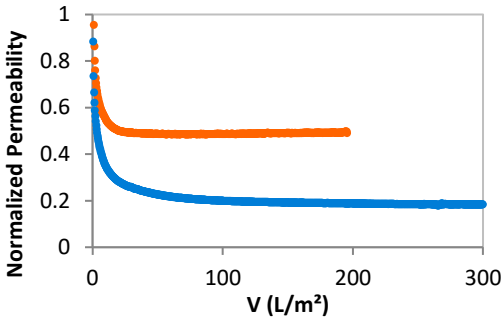

Figure A 18: Experiment No. 18

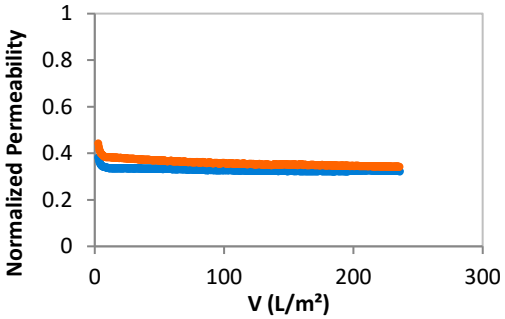

Figure A 19: Experiment No. 19

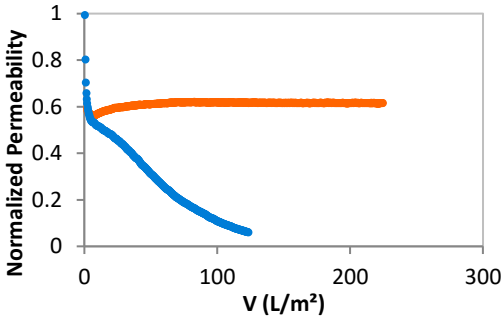

Figure A 20: Experiment No. 20

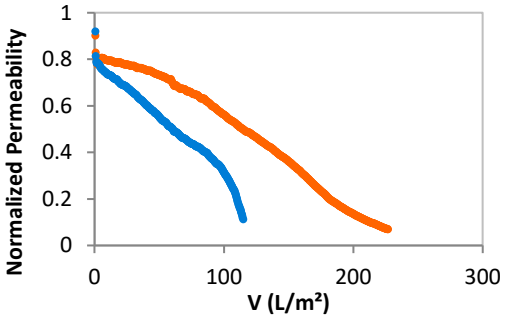

Figure A 21: Experiment No. 21

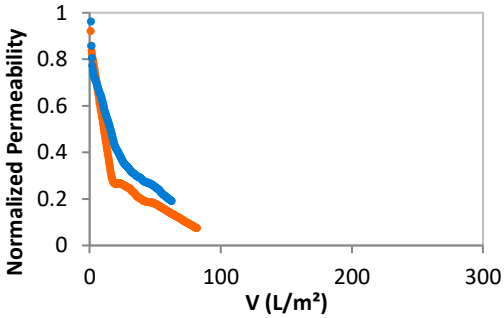

Figure A 22: Experiment No. 22

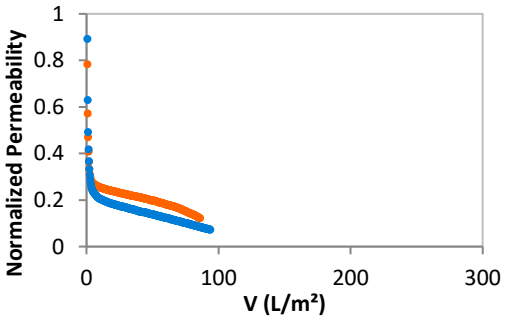

Figure A 23: Experiment No. 23

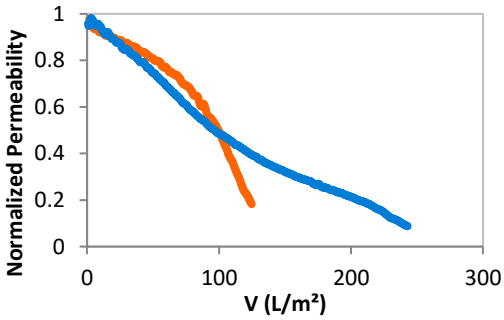

Figure A 24: Experiment No. 24

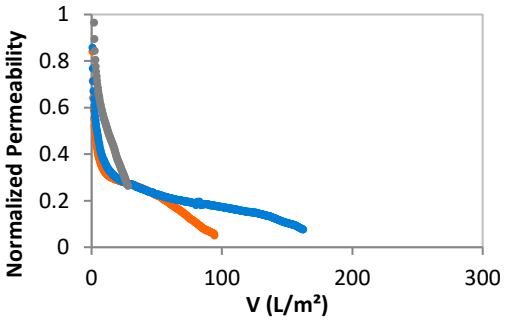

Figure A 25: Experiment No. 25

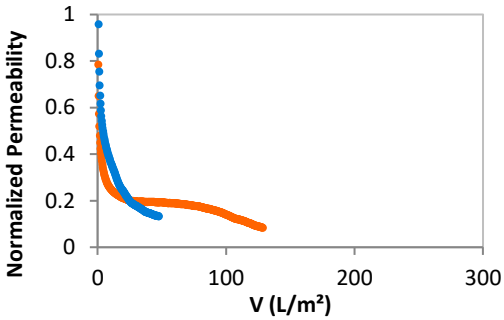

Figure A 26: Experiment No. 26

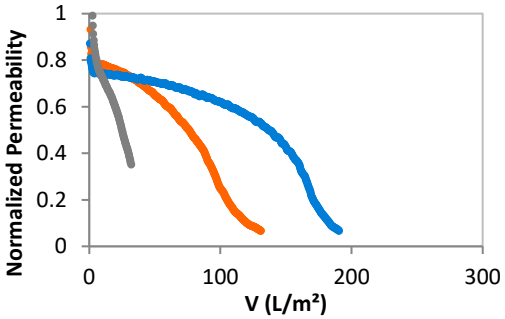

Figure A 27: Experiment No. 27

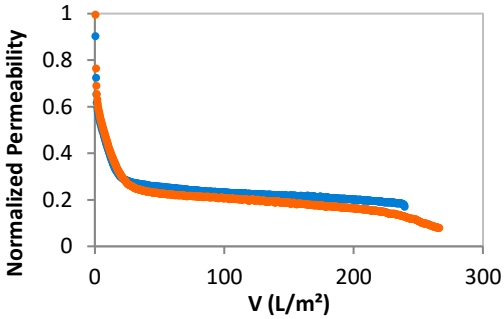

Figure A 28: Experiment No. 28

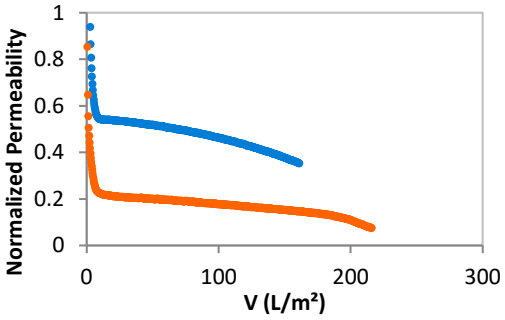

Figure A 29: Experiment No. 29

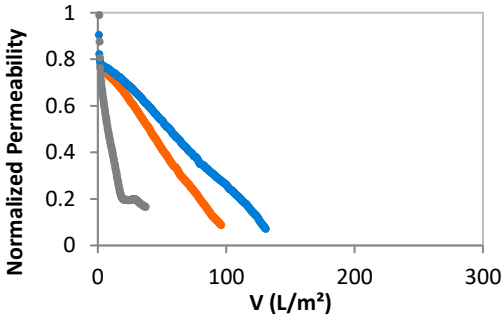

Figure A 30: Experiment No. 30

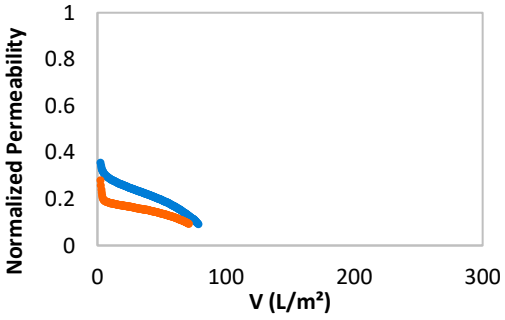

Figure A 31: Experiment No. 31

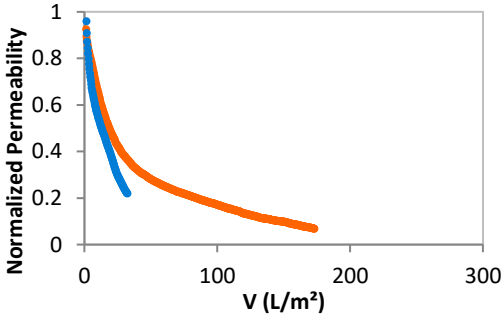

Figure A 32: Experiment No. 32

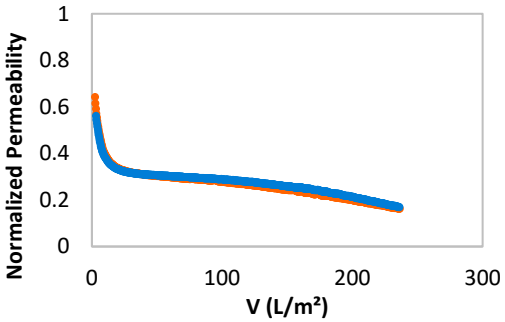

Figure A 33: Experiment No. 33

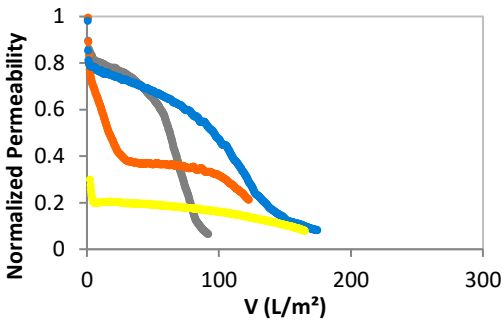

Figure A 34: Experiment No. 34

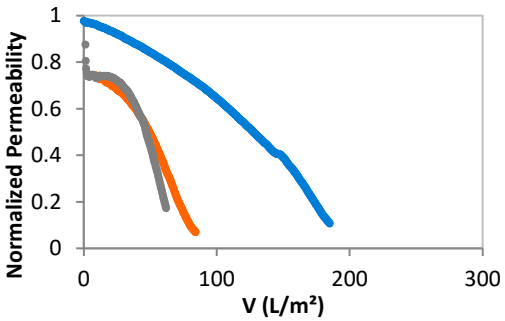

Figure A 35: Experiment No. 35

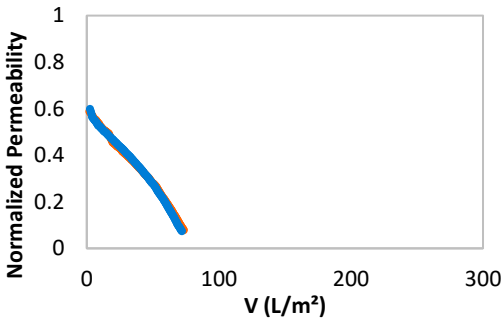

Figure A 36: Experiment No. 36

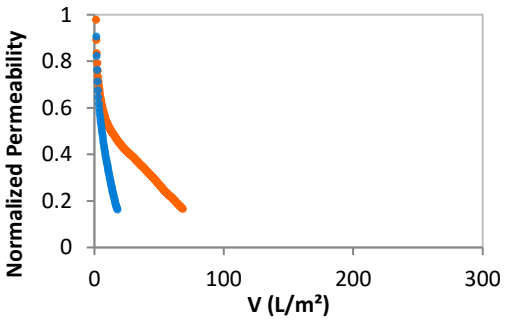

Figure A 37: Experiment No. 37

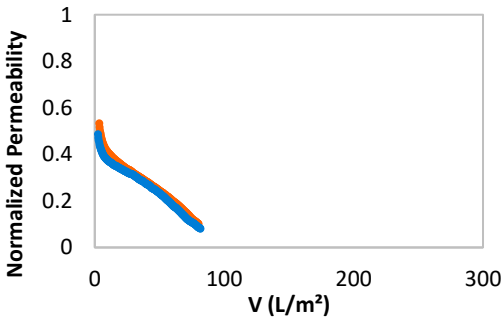

Figure A 38: Experiment No. 38

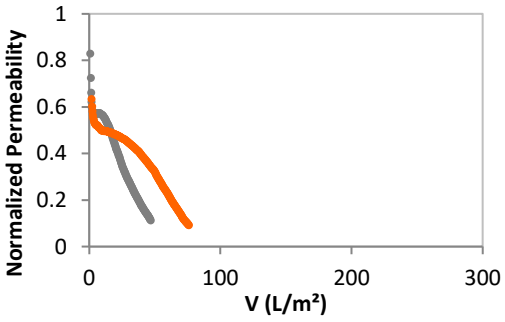

Figure A 39: Experiment No. 39

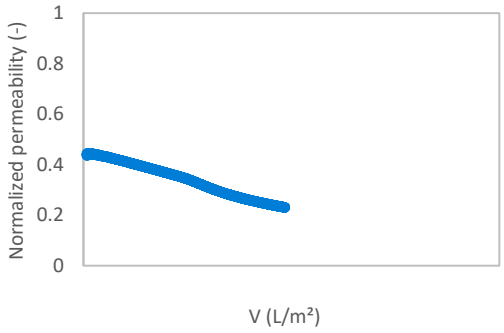

Figure A 40: Experiment No. 41

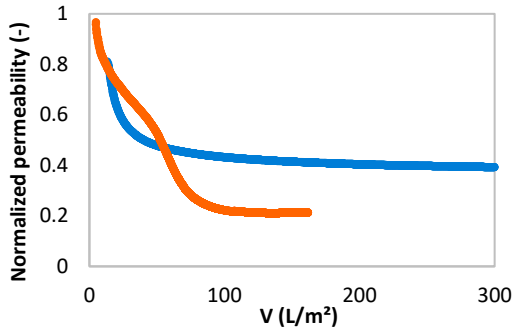

Figure A 41: Experiment No. 42

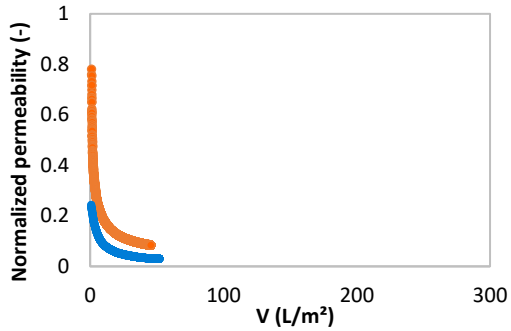

Figure A 42: Experiment No. 43

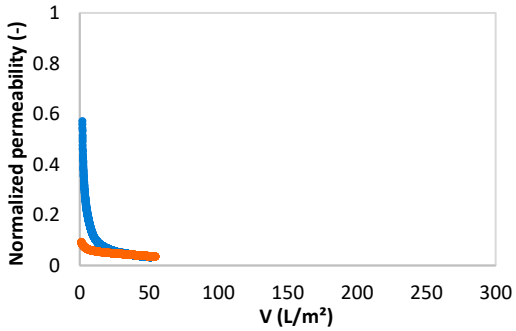

Figure A 43: Experiment No. 44

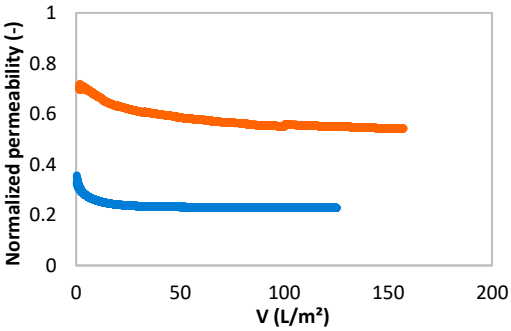

Figure A 44: Experiment No. 45

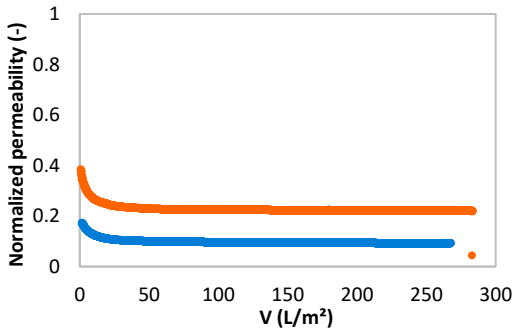

Figure A 45: Experiment No. 46

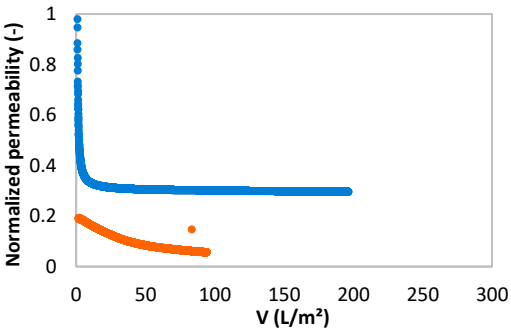

Figure A 46: Experiment No. 47

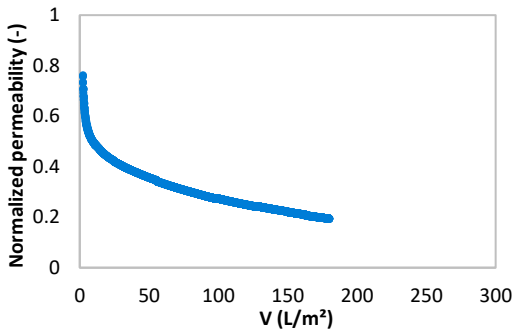

Figure A 47: Experiment No. 48

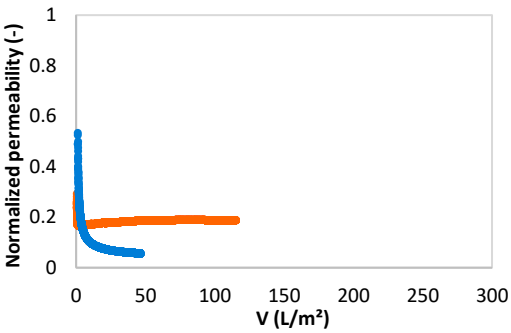

Figure A 48: Experiment No. 49

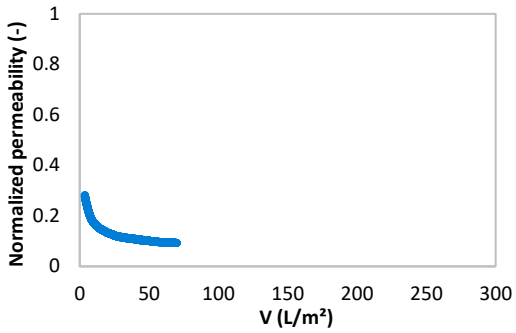

Figure A 49: Experiment No. 50

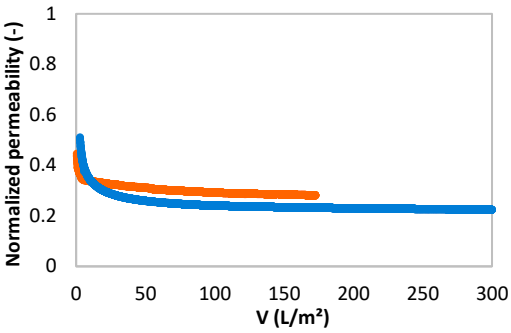

Figure A 50: Experiment No. 51

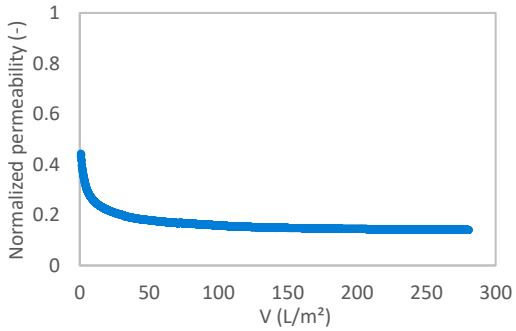

Figure A 51: Experiment No. 52

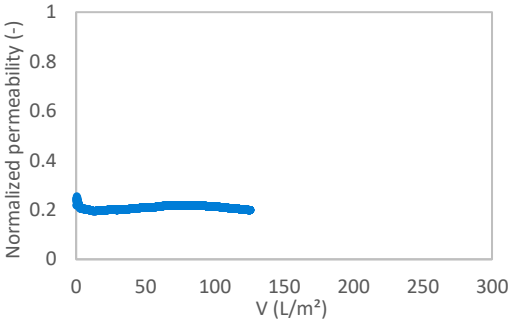

Figure A 52: Experiment No. 53

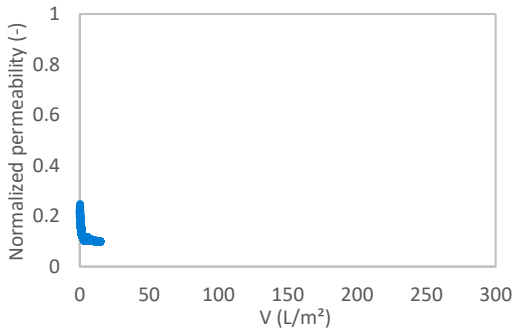

Figure A 53: Experiment No. 55

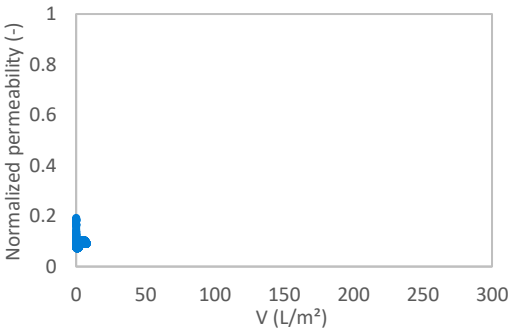

Figure A 54: Experiment No. 56

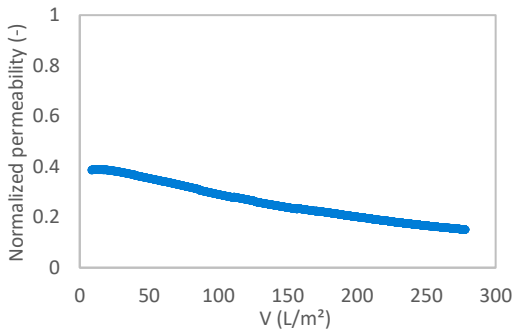

Figure A 55: Experiment No. 57

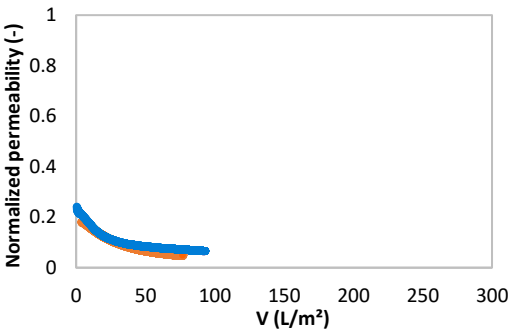

Figure A 56: Experiment No. 58

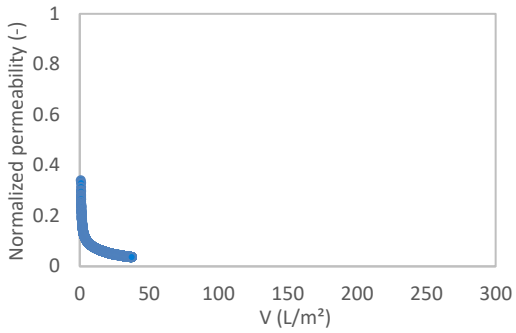

Figure A 57: Experiment No. 59

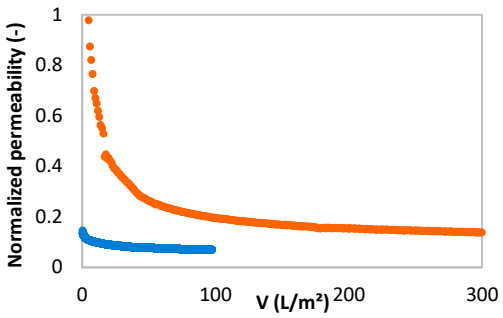

Figure A 58: Experiment No. 60

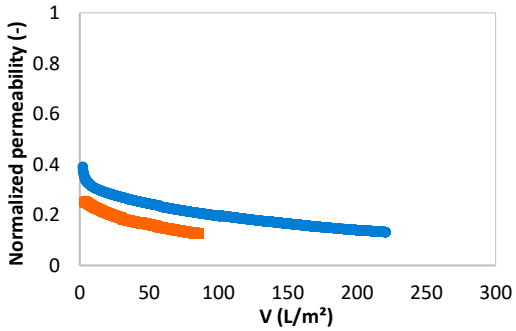

Figure A 59: Experiment No. 61

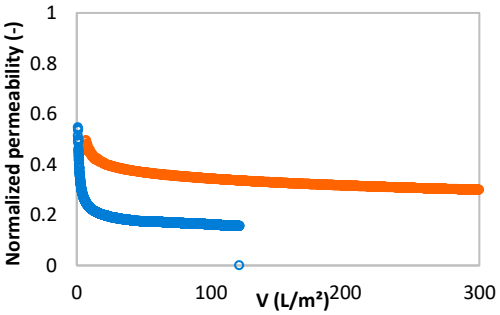

Figure A 60: Experiment No. 62

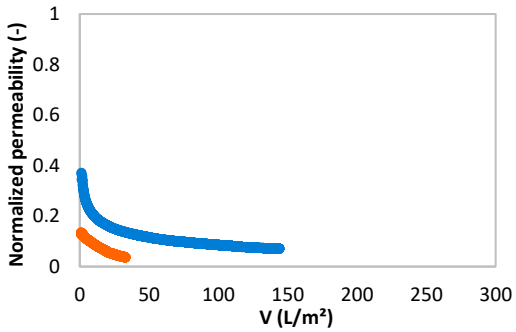

Figure A 61: Experiment No. 64

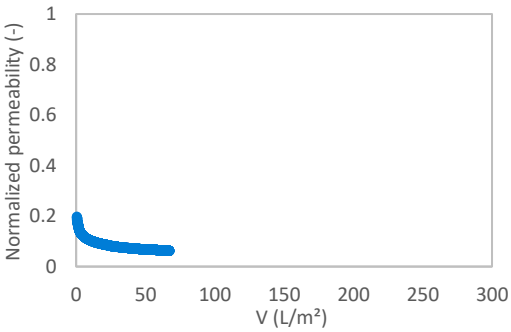

Figure A 62: Experiment No. 65

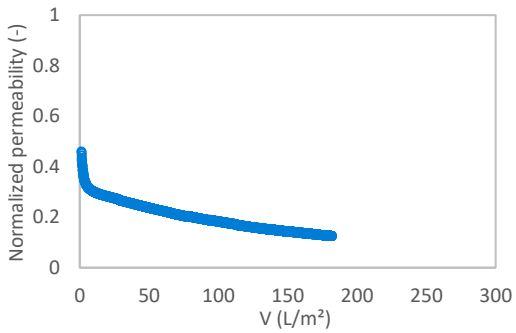

Figure A 63: Experiment No. 66

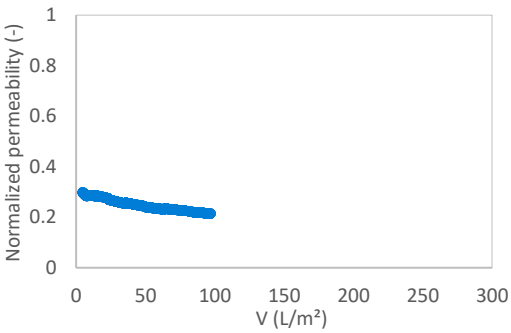

Figure A 64: Experiment No. 67

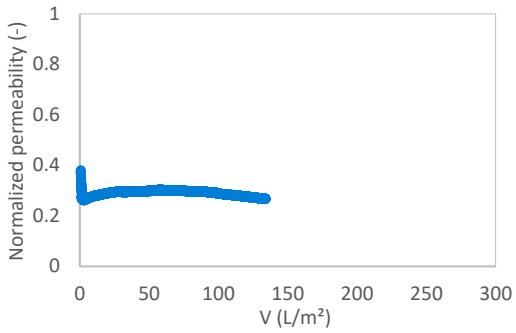

Figure A 65: Experiment No. 68

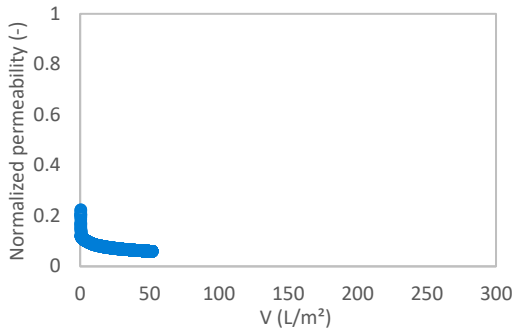

Figure A 66: Experiment No. 70